Atomic Energy Control Board
P O Box 1046
Ottawa Canada
K1P 5S9

Commission de contrôle de l'énergie atomique
C P 1046
Ottawa Canada
K1P 5S9

INFO-0155

GEOCHEMICAL ANALYSIS OF CORE FROM A GEOTHERMAL ANOMALY

by

B. Haverslew and H.Y. Tammemagi
RE/SPEC Ltd.

A research report prepared for the
Atomic Energy Control Board
Ottawa, Canada

April 1985

Canada

Research report

GEOCHEMICAL ANALYSIS OF CORE
FROM A GEOTHERMAL ANOMALY

ABSTRACT

A mild geothermal area in western Montana, USA, has been studied, as a natural analog, to learn about the effects that long-term heat generated by a repository containing spent nuclear fuel might have on the surrounding rock mass. The results of previous geological, geophysical and hydrogeological studies are briefly summarized. Extensive petrological studies have been undertaken on core samples obtained from a 2 km deep borehole drilled into the Empire Creek Stock. These include a detailed petrographic study, x-ray diffraction analyses, scanning electron microscope and electron microprobe analyses, porosity and permeability measurements, oxygen isotope analyses, uranium disequilibrium analyses and K-Ar age determinations. The implications to deep burial of nuclear wastes are discussed.

RÉSUMÉ

Une région géothermique tempérée située dans l'ouest du Montana aux États-Unis a été étudiée en tant que modèle analogique naturel, et ce en vue de déterminer les effets éventuels de la chaleur prolongée produite par un dépôt de combustible nucléaire irradié sur la masse rocheuse environnante. Les résultats d'études géologiques, géophysiques et hydrogéologiques antérieures sont résumés dans l'ouvrage. Des études pétrologiques poussées ont été entreprises aux fins d'analyse d'échantillons prélevés dans un trou de sonde de 2 kilomètres de profondeur creusé dans l'Empire Creek Stock. Ces études comprennent une étude pétrographique détaillée, des analyses radiologiques de diffraction, des analyses au microscope électronique à balayage et à la microsonde de Castaing, des mesures de la porosité et de la perméabilité, des analyses des isotopes d'oxygène, des analyses du déséquilibre de l'uranium et la détermination de l'âge du potassium et de l'argent. L'ouvrage traite également des conséquences de l'enfouissement profond des déchets nucléaires.

DISCLAIMER

The Atomic Energy Control Board is not responsible for the accuracy of the statements made or opinions expressed in this publication, and neither the Board nor the authors assume liability with respect to any damage or loss incurred as a result of the use made of the information contained in this publication.

	Page
ABSTRACT	i
TABLE OF CONTENTS	ii
A. INTRODUCTION	1
B. OVERVIEW OF GEOTHERMAL SYSTEMS	4
1. Geothermal Review	4
2. Geothermal Energy Research	7
3. Hydrothermal Convection in Igneous Rocks	8
C. GEOLOGICAL SETTING	10
1. Regional Geology	10
2. Local Geology	10
D. REVIEW OF GEOTHERMAL INVESTIGATIONS	16
E. STUDIES OF DRILL CORE FROM THE EMPIRE CREEK STOCK	17
1. Petrography and Petrochemistry	17
2. Fracture and Alteration Mineralogy	21
3. Porosity and Permeability	25
4. Fluid Inclusions	26
5. Oxygen Isotopes	28
6. Potassium-Argon Age Dating	31
7. Uranium Disequilibrium Analyses	33
F. DISCUSSION/SYNTHESIS	35
1. Introduction	35
2. Emplacement of the Empire Creek Stock	35
3. Post Magmatic Alteration	36
4. Subsequent Alteration	37
5. Summary	40
6. Recommendations	42
G. REFERENCES	44
H. ACKNOWLEDGMENTS	48
APPENDICES:	
DETAILED BOREHOLE LITHOLOGY	A1
PHOTOMICROGRAPHS OF THIN SECTIONS OF EMPIRE CREEK GRANITE	B1

A. INTRODUCTION

An accurate prediction of the long-term performance and safety of a nuclear waste repository is seriously complicated by the long time periods which will be involved (tens of thousands of years) as well as the inherent complexity of the repository/geology/groundwater system. Therefore, the study of natural phenonema which imitate anticipated repository behaviour, the so-called natural analogues, is increasingly being recognized as an important complement to mathematical models.[1,2]

A specific concern for disposal of spent fuel in granite is the effect that the heat will have on the rock mass and hydrogeologic system. Current repository concepts being developed by Atomic Energy of Canada Ltd. (AECL) predict that temperatures of approximately 80 to 100°C will be sustained in the region of a spent fuel repository for approximately 20,000 years.[3,4] In contrast, temperatures near a reprocessed waste repository will dissipate in a few hundred years. It is not clear how the rock mass will react to elevated temperatures over a period of time which approaches the geologic time scale. To develop a better understanding, this study has investigated a mild geothermal area in Montana as a possible natural analogue to a repository system.

The geothermal anomaly near Marysville, Montana was discovered in 1965[5] and was unusual in that it was "blind", showing no surface manifestations such as fumaroles, hotsprings, etc. The anomaly was extensively explored from 1972-1974 in order to assess its potential as an economic geothermal energy resource.[6,7,8]

The exploration activities included geological mapping, geophysical surveys, and the drilling of a 2.1 km deep borehole. The studies revealed that the anomaly was related to a Cenozoic granite pluton, the Empire Creek Stock, which intrudes metamorphosed Precambrian sediments. The deep borehole penetrated an extensive hydrothermal zone; however, the temperatures encountered never exceeded 100°C and, thus, were too low to support commercial energy extraction

and the project was terminated.

Although unsuitable for energy exploitation, the Marysville anomaly was thought to be well suited to be an analogue for a nuclear waste repository for the following reasons: (a) temperatures in the ground are approximately the same as those anticipated in a repository (95°C maximum) and (b) the anomaly is associated with a granitic pluton.

In addition, a considerable amount of information is available from the geothermal exploration. For example, the deep borehole extends considerably deeper in a pluton than any boreholes drilled in nuclear waste disposal programs.

The present study was preceded by a literature review of the Marysville geothermal anomaly from a nuclear waste disposal perspective [9]. That review hypothesized that the active groundwater circulation, the alteration of the rock mass, and the relatively permeable fracture zones in the Empire Creek stock may have been, at lease in part, caused by the thermal anomaly. It is well known that igneous rocks, both intrusive and extrusive, in geothermal regions may develop significant fracture permeability and, thus, increase their capability to transmit heat by groundwater convection. Many questions require resolution, however, before the Marysville anomaly may be used as an analogue. For example, is the present groundwater circulation/permeability associated with thermal conditions similar to a spent fuel repository or were they caused by considerably higher temperatures acting over much longer periods? Is the highly fractured and permeable nature of the Empire Creek stock a result of the original emplacement or is it due to subsequent events? Etc.

Eleven core samples and numerous cuttings of the Empire Creek stock had been procured at approximately regular intervals through the 2.1 km deep geothermal borehole. The main objective of this study was to perform a detailed petrological and geochemical analysis of these cores and cuttings. The purpose was to establish the petrologic character and genesis of the stock and to determine the history of the hydrothermal mineralization and related

alteration. In particular, it was sought to determine the number, duration and temperatures of the thermal pulse(s) which caused mineralization and alteration. The underlying objective was that by employing these methods, in conjunction with the information that is already available, it would be possible to resolve the queries raised in the previous paragraph and thereby to draw relevant conclusions from this natural analogue regarding implications of long-term heat to repository containment.

To address this idea this report is organized in the following manner: A comparison to other geothermal areas including a discussion of thermal conditions in western North America is provided in Section B. The local and regional geologic setting of the Empire Creek stock and related geothermal anomaly is reviewed in Section C. A brief description of the original geothermal investigations is presented in Section D in order to provide necessary background for this study. Section E describes the petrological studies such as fluid inclusions studies, uranium disequilibrium determinations, porosity measurements, etc. which were performed to investigate the character of the ECS and of the thermal pulses(s). Section F presents a synthesis of the results and discusses their relevance to nuclear waste disposal. Conclusions and recommendations are also presented in this section.

B. OVERVIEW OF GEOTHERMAL SYSTEMS

1. Geothermal Review

This section will briefly review the geothermal regime of the earth and then will focus on the heat flow conditions in western North America. The objective is to provide an understanding of heat transfer mechanisms in the earth, particularly of the role that groundwater plays; and also to provide a regional background or perspective so that the Marysville geothermal anomaly may be better understood. This general discussion will also provide background information which may be useful in the selection and/or study of geothermal areas as analogues to nuclear waste repositories. It will be seen that convective heat transport by hydrothermal systems is a key factor. However, our understanding of the complex interactions between geologic formations, sources of thermal energy, and groundwater is extremely limited, and there is still much to learn before long-term predictions can be made with confidence.

The earth is dissipating heat at a worldwide average rate of about 60 mW/m^2. The majority of this heat originates from the radioactive decay of a number of radioactive nuclides (primarily ^{40}K, U, Th) found in the crust and upper mantle. Since this energy source drives plate tectonics, continental drift, mountain building, etc., it is not surprising that regional heat flow variations can be correlated with tectonic regimes and processes. (It is interesting to note that the forces which sculpt our mountains and valleys are caused by a great nuclear power plant -- the earth). In the earth's oceans, heat flow is generally inversely related to the age of the oceanic crust, that is, its time of cooling since formation. On the continents, heat flow generally correlates with physiographic (i.e. tectonic) provinces, with shields having the lowest geothermal gradients while the highest heat flows are found in areas of recent volcanics, which generally occur near plate boundaries.

The heat flow regime of western North America has been the subject of several studies [5,10]. A simplified heat flow map is shown in Figure 1 where it is seen that distinct regional high heat flow anomalies are associated with the

FIGURE 1 - REGIONAL HEAT FLOW IN WESTERN USA AFTER REF. 10. CONTOUR UNITS ARE mW/m^2. ABBREVIATIONS ARE ECS for EMPIRE CREEK STOCK, SRP for SNAKE RIVER PLAIN, BMH for BATTLE MOUNTAIN HIGH, EL for EUREKA LOW, SN for SIERRA NEVADA AND RGR for RIO GRANDE RIFT.

Rio Grande rift and a large area encompassing the Battle Mountain High and the Snake River Plain. The Yellowstone thermal area is found in the latter area, and the Marysville area of this study lies about 200 km to the north of it. Distinctive lows are associated with the Eureka Low and Sierra Nevada province. It should be stressed that heat flow data is still relatively sparse, and the boundaries shown in Figure 1 are subject to future revision.

Heat flow measurements in the field (both on the oceans and on land) are based on the assumption that heat transfer is occurring conductively, and regions where convective heat transfer might be occurring have generally been avoided because of their associated complications. About 10 to 15 years ago, it was realized that convective hydrothermal systems were associated with sea floor spreading centers and actually dominate not only the heat budget (about 20 percent of the earth's total heat loss!) but also the geochemical mass balance at mid-ocean ridges [11]. Igneous rocks, which were previously considered to be essentially impervious are, in reality, fractured and are transporting significant quantities of water and heat. Steady state models indicate that fractures of the order of a few millimetres wide can carry a substantial convective flow [12].

The significance of groundwater convection for continental heat flow has also begun to be increasingly recognized. In a milestone paper, Lachenbruch and Sass [10], provide equations for estimating the effect of convective heat transport and discuss the impact it has on regional heat flow.

It is interesting to note that both the Basin and Range province (high heat flow) and the mid-ocean ridges, where convective hydrothermal systems are active, are regions of crustal spreading, that is, zones of horizontal tensile stress. Clearly, a tensile stress field is a contributing factor in the formation of conduits for water circulation. It should be noted that in the Canadian Shield, the horizontal stress field, in contrast, is compressive and anomalously high [13].

2. Geothermal Energy Research

As part of the search for alternative energy sources, the U.S. government has sponsored considerable research into geothermal energy. These investigations have included the mapping and evaluation of anomalous heat flow in the U.S.A.[14] as well as intensive studies of specific geothermal areas. For example, the following areas have been thoroughly studied and documented and may provide useful information to the Canadian nuclear waste disposal programs regarding long term effects of heat on rock:

- The Coso geothermal area is located in the Coso Range in southeast California and has been studied by the U.S. Geological Survey and others[15].
- The Roosevelt Hot Springs thermal area is located in southwestern Utah[16] and may be of interest since it is located in a Tertiary granite pluton.
- Undoubtedly, the best known geothermal anomaly is the Yellowstone geothermal area, in northwest Wyoming. Situated in recent volcanic terrain, it features dramatic geyser and hot spring activity[17].
- The Raft River geothermal area in southeastern Idaho is under investigation for the generation of electricity from an intermediate-temperature reservoir and has been thoroughly studied[18].
- The Imperial Valley, California, is the site of commercial geothermal energy extraction and has been the subject of considerable investigation[19]. A number of geothermal fields occur in this region of extensional tectonics and one of them, the Salton Sea geothermal field, has been investigated from a repository analogue viewpoint[2].

A special mention should be made of the dry hot rock geothermal project being undertaken by Los Alamos Scientific Laboratory in the Jemez Mountains of northern New Mexico. The concept is to drill two deep boreholes (about 2 to 4 km deep) into an impermeable granitic rock with a high geothermal gradient. The bottoms of the boreholes are connected by hydraulic fracturing and then cold water is pumped down one hole, allowed to heat up naturally and then pumped up

the other borehole. The concept has passed the feasibility evaluation phase[20]. Two boreholes, each 2650 m deep, have been sunk and considerable research has been done in assessing permeability of the rock mass, developing hydrology instrumentation and geophysical techniques, etc. Unfortunately, the investigations are not particularly relevant to this study since a heat sink rather than a heat source is involved and, therefore, the physical phenomena, e.g., thermal shrinkage, are different. However, an abundance of other relevant information may be gleaned for the Canadian nuclear waste disposal program regarding such matters as the efficacy of geophysical techniques, rock/water conditions at and below repository depth, hydrologic measurement techniques, and rock alteration.

Within Canada, an investigation into geothermal resource potential was initiated by the federal government in 1972. The potential for geothermal power development is restricted to the Cordillera of British Columbia, the Yukon and western Alberta which forms part of the seismically active circum-Pacific orogenic belt[21]. The Garibaldi volcanic belt has been singled out for particular attention. It consists of the volcanic roots of a volcanic front related to the subduction of the Juan de Fuca plate. Considerable research has been carried out near Meager Mountain (about 120 km north of Vancouver) under the sponsorship of the federal government and B.C. Hydro[22]. Because of the young, tectonically-active region, the rock types, and the variable topography, it is questionable whether the area would serve as a useful natural analogue to the Canadian repository program.

3. Hydrothermal Convection in Igneous Rocks

The preceding review of geothermal areas illustrates the importance of hydrothermal convection in the dissipation of heat through geological systems. In igneous rocks, convective ground water motion taking place through fractures is relatively commonplace in regions where there are sources of heat, such as in and around mid-ocean ridges. The specific details of how the flow conduits (i.e. fractures) form and what conditions are required for the initiation of

convective flow are not well understood. The process is complex and includes such factors as the ambient stress conditions, rock mass properties (strength, pre-existing fracture sets, etc.), temperatures, temperature gradients, the chemistry of the rock mass, fracture filling materials and groundwater, and time. A quantitative theory combining these factors does not exist at the present time and it is clear that it is impossible to predict whether a nuclear waste repository located in a carefully selected granitic pluton will result in a convective hydrothermal system such as is associated with geothermal systems.

C. GEOLOGICAL SETTING

1. Regional Geology

The Marysville "blind" geothermal anomaly is located about 30 km northwest of Helena, Montana, and 4.5 km west of the old gold mining town of Marysville (Figure 2). It is in an area of the Cordilleran Orogen which has been affected variously by periods of volcanism, plutonism, folding, thrusting, normal faulting and/or seismicity since Late Cretaceous time.

The regional geology of this part of Montana is dominated by the Boulder batholith, a large composite plutonic mass which has an aerial exposure of over 6,000 km^2 (2200 mi^2) from 5 km south of Helena, Montana, to 30 km south of Butte, Montana. The Boulder batholith is made up of at least a dozen calc-alkalic plutons which range in composition from syenogabbro to alaskite with a dominant composition of quartz monzonite to granodiorite. Many genetically related and compositionally similar satellitic plutons flank the main body of the batholith. The batholith and satellitic stocks intruded and metamorphosed sedimentary rocks of Precambrian to Mesozoic age, and intrude the genetically related contemporaneous Elkhorn Mountains volcanics[23]. Radiometric age dating indicates that the main body of the Boulder batholith was emplaced during the time span from 78 to 72 million years ago. Intrusion of the batholith was accompanied and followed by folding and thrusting on a regional scale. Renewed volcanic activity occurred regionally at about 50 million years ago and 40 - 37 million years ago.

Normal faulting is responsible for much of the present physiography of the region, and the Helena area has experienced episodes of strong seismic activity in recent times [24].

2. Local Geology

The main features of surficial bedrock geology in the area of the Marysville Geothermal anomaly are the contact metamorphosed sedimentary

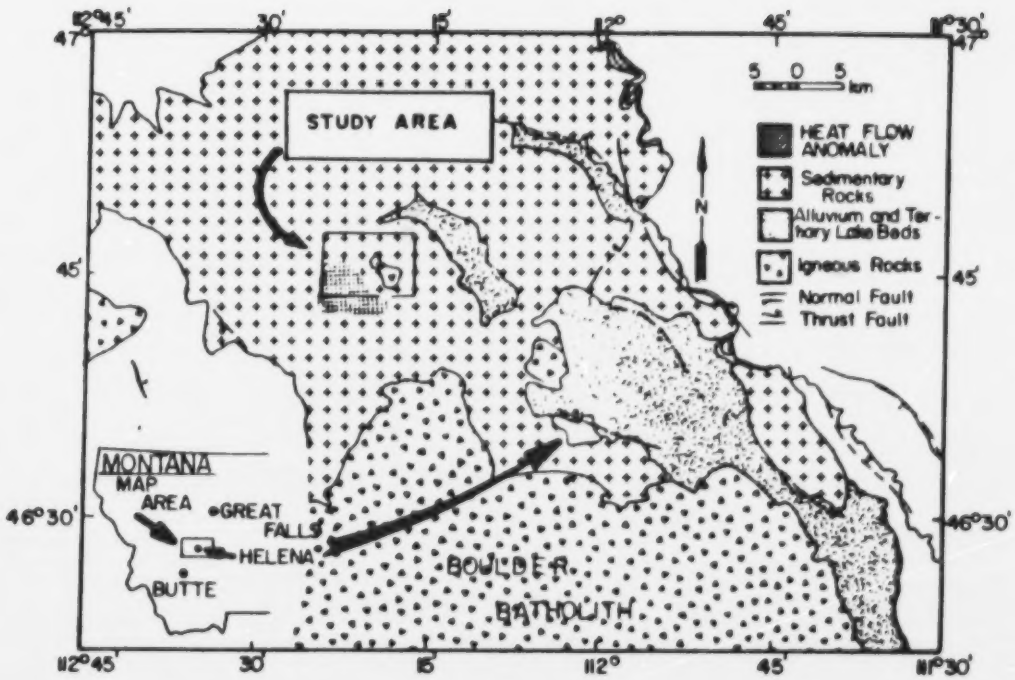

FIGURE 2 - GENERALIZED GEOLOGIC MAP OF THE HELENA, MONTANA REGION (AFTER FRIEDLINE ET AL[24]).

rocks of the Precambrian Belt series and the Marysville granodiorite stock, a satellitic intrusion of the Boulder batholith (Figure 3).

The Belt Series formations with the greatest areal extent in the vicinity of the Marysville geothermal anomaly are the Helena limestone, consisting mainly of siliceous limestone and dolomite, and the underlying biotite-rich siliceous to calcareous Empire shale. The Empire shale is underlain by the purple to grey-green argillite of the Spokane shale, and the Helena limestone is overlain successively by the red to maroon Marsh shale and the Greenhorn and Black Mountain quartzites. The Helena limestone and the Empire shale have been contact metamorphosed to calc-silicate hornfels over much of the area.

The complex igneous history of the Marysville area is summarized in Table 1 The oldest igneous rocks are microdiorite sills in the upper part of the Empire shale of probable Precambrian age. The Marysville granodiorite is the next dated igneous event at 78 my,[25] representing an early satellitic phase of the Boulder batholith. Southwest of the Marysville granodiorite, mineral exploration drilling has intersected the Bald Butte and Empire Creek stocks which are interpreted as being adjacent to each other at depth and may, in fact, be a single stock (Figure 4). The Bald Butte and Empire Creek stocks have been dated at 49 my and 40 my respectively [7] although Ratcliffe (1984, personal communication) noted that a 40 my age has also been reported for the Bald Butte stock. Farther to the southwest, remnants of a previously more extensive suite of rhyolitic volcanics, the Hope Creek volcanics, are dated at 37 my and probably represent the extrusive equivalent of the Bald Butte and/or Empire Creek porphyries.

The main structural feature of the area is a dome in the sedimentary rocks, the core of which is expressed by the outcrop area of the Empire shale, the oldest unit exposed in the immediate area. The dome in the Empire shale corresponds closely with both the geothermal anomaly and other contact-metamorphic zones which are interpreted as being related

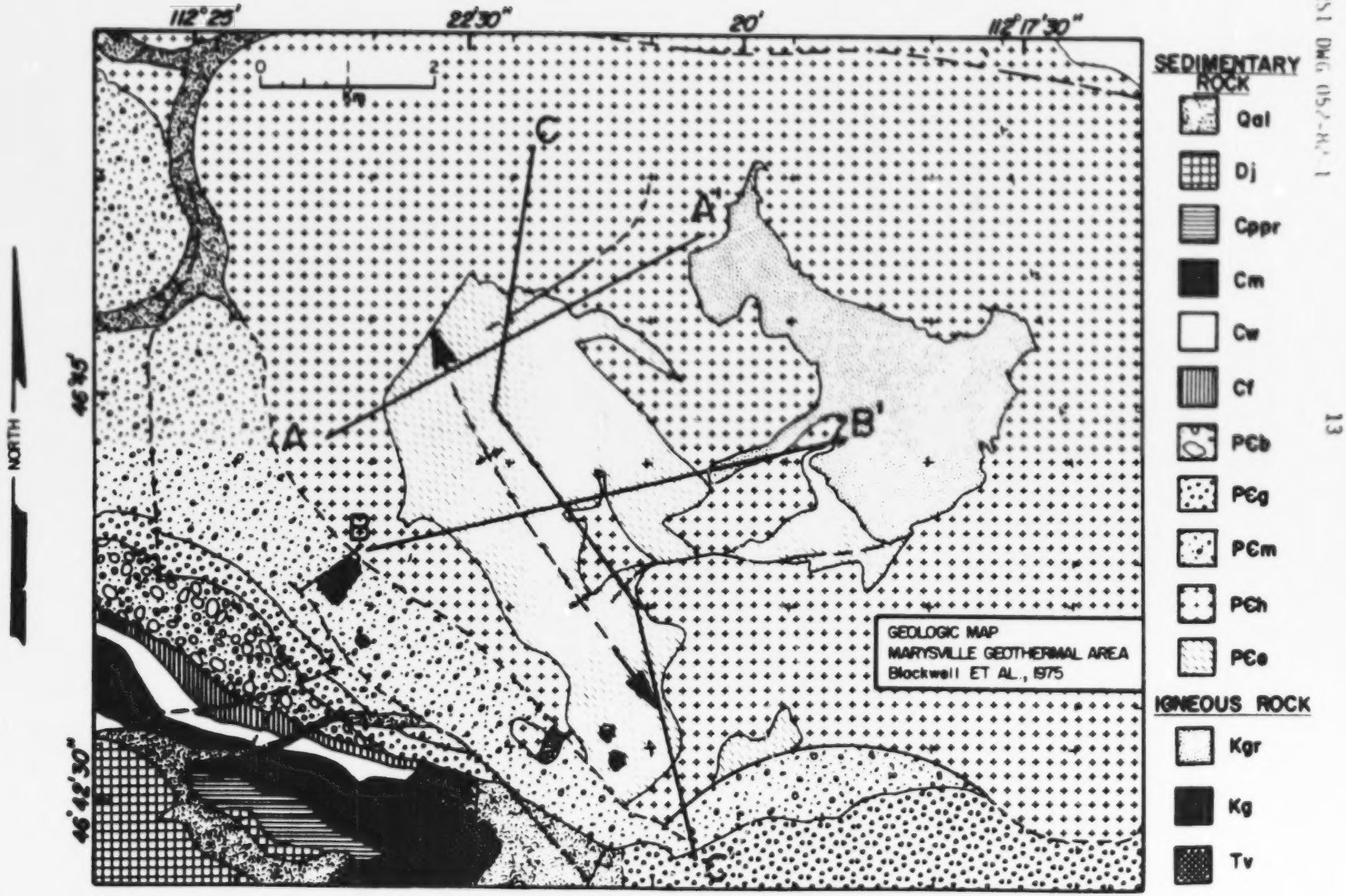

FIGURE 3 - GEOLOGIC MAP OF THE MARYSVILLE GEOTHERMAL AREA (FROM BLACKWELL ET AL[26]).

RSI DWG 05/-88-1

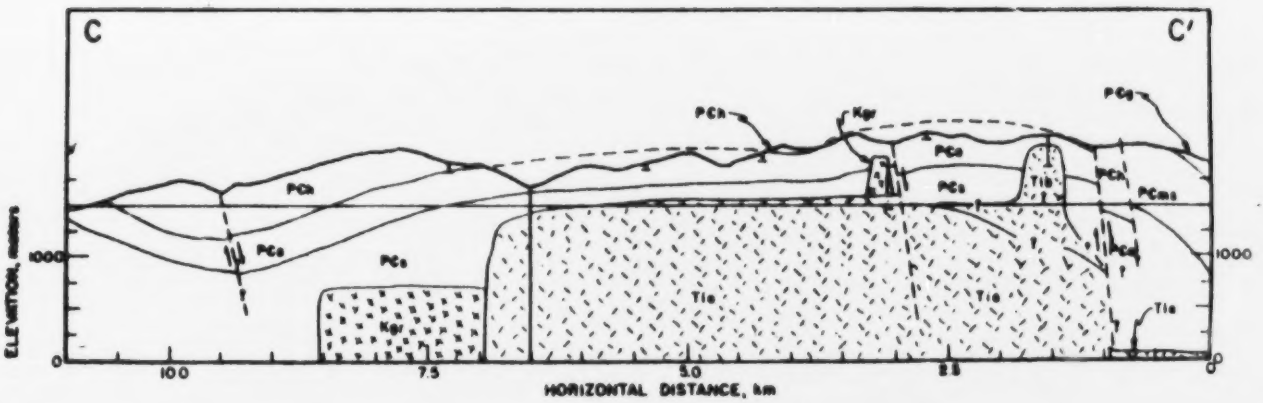

FIGURE 4 - CROSS SECTION OF THE MARYSVILLE GEOTHERMAL AREA.
LOCATION OF CC[1] IS SHOWN IN FIGURE 3.
Kgr = MARYSVILLE STOCK, Tie = EMPIRE CREEK STOCK,
Tib = BALD BUTTE STOCK (FROM BLACKWELL ET AL[26]).

to the intrusion of the Empire Creek Stock[26].

Some faulting in this area is demonstrably later than the intrusion of the granodiorite, and microearthquake activity has been recorded southeast of the geothermal anomaly[24].

Table 1 - Major Igneous Events in the Marysville, Montana Area

Event	Age
Intrusive Causing the Geothermal Anomaly	Quaternary or Recent (20-50k yr)
Rhyolite Flows	Oligocene (37 Ma)
Empire Creek Stock	Oligocene (40 Ma)
Hornblende Diorite Dikes and Sills	Eocene (48 Ma)
Bald Butte Stock	Eocene (49 Ma or 40 Ma)
Marysville Stock	Cretaceous (79 Ma)
Microdiorite Sills	Precambrian (?)

D. REVIEW OF GEOTHERMAL INVESTIGATIONS

The geothermal investigations carried out in the Marysville area in 1972-74 provide a case history with much useful information for nuclear waste disposal. Only a brief description is provided here in order to provide background, and the interested reader is referred to Tammemagi et al.[9] for a more comprehensive report.

A number of hydrogeological studies were done as part of the geothermal project in the Marysville area [8,27]. Significant fracture zones with groundwater flow were encountered at approximately 460 m, 550 m, 1000 m, 1400 m, 1800 - 1900 m and 2040 - 2070 m in the deep borehole. There was a flow of about 16 l/s from the 1000 m zone to the 2040 - 2070 zone until the bottom of the drill hole was plugged with cement. There appears to be good vertical hydraulic connectivity between major subhorizontal permeable zones which permits convective groundwater motion to occur. Water samples were collected from the deep borehole. Samples from near surface (<171m) are similar to the shallow groundwater in the area which is predominantly a calcium bicarbonate water with a median chloride concentration of about 8 mg/l. Deeper samples are distinctly different generally demonstrating a dilute sodium-bicarbonate-sulfate water with a relatively high fluoride content and are similar to thermal springs in the region.

^{18}O analyses indicated little or no shift from the meteoric water line relating ^{18}O to ^{2}H in Western Montana[8], suggesting that the temperatures of the geothermal source are below 150°C and the circulating waters are of relatively recent meteoric origin. The temperatures calculated by the SiO_2 and Na-K-Ca geothermometer methods are 110-130° and 165-180°C respectively.

A comprehensive suite of geophysical exploration surveys was used in the geothermal project[6,7,8]. The methods employed included heat flow, gravity, electrical resistivity, magnetotellurics, magnetics, seismic ground noise and borehole logging. Important information arising from these surveys was that:

1) Heat flow measurements in shallow boreholes yielded geothermal gradients up to 240°C/km and heat transfer of up to 800 mW/m^2, values which are approximately 10 times the world average.
2) Temperature logs recorded in the deep borehole (Figure 5) indicated that conductive heat transfer was occurring in the upper region whereas convective heat transfer was occurring in the middle and lower regions.
3) The surface geophysical surveys did not predict the vigorous groundwater flow system occurring in the Empire Creek Stock.
4) An intriguing contrast exists between the adjacent Empire Creek Stock and Marysville Stock. The latter showed a normal heat flow and a normal gravity field, had a large magnetic anomaly and a high eletrical resistivity. The Empire Creek Stock in contrast had a high heat flow anomaly, a negative gravity anomaly, normal magnetic field and high electrical resistivity.

E. STUDIES OF DRILL CORE FROM THE EMPIRE CREEK STOCK

Eleven of the fifteen cores taken from the deep drill hole are from the granite of the Empire Creek Stock (Figure 5). Preliminary studies of these core samples were reported by McSpadden et al[8]. The present study has augmented the previous work by performing a detailed petrographic study of over 60 thin sections, x-ray diffraction analyses of cuttings, veins and alteration minerals, scanning electron microscope (SEM) studies and electron microprobe (EMP) analyses, porosity and permability measurements, oxygen isotope analyses, uranium disequilibrium analyses, and K-Ar age determinations.

1. Petrography and Petrochemistry

This section presents a summary of the detailed petrographic descriptions of each core which are provided in Appendix A. Photomicrographs of thin sections illustrating many of the features described in this section are in Appendix B.

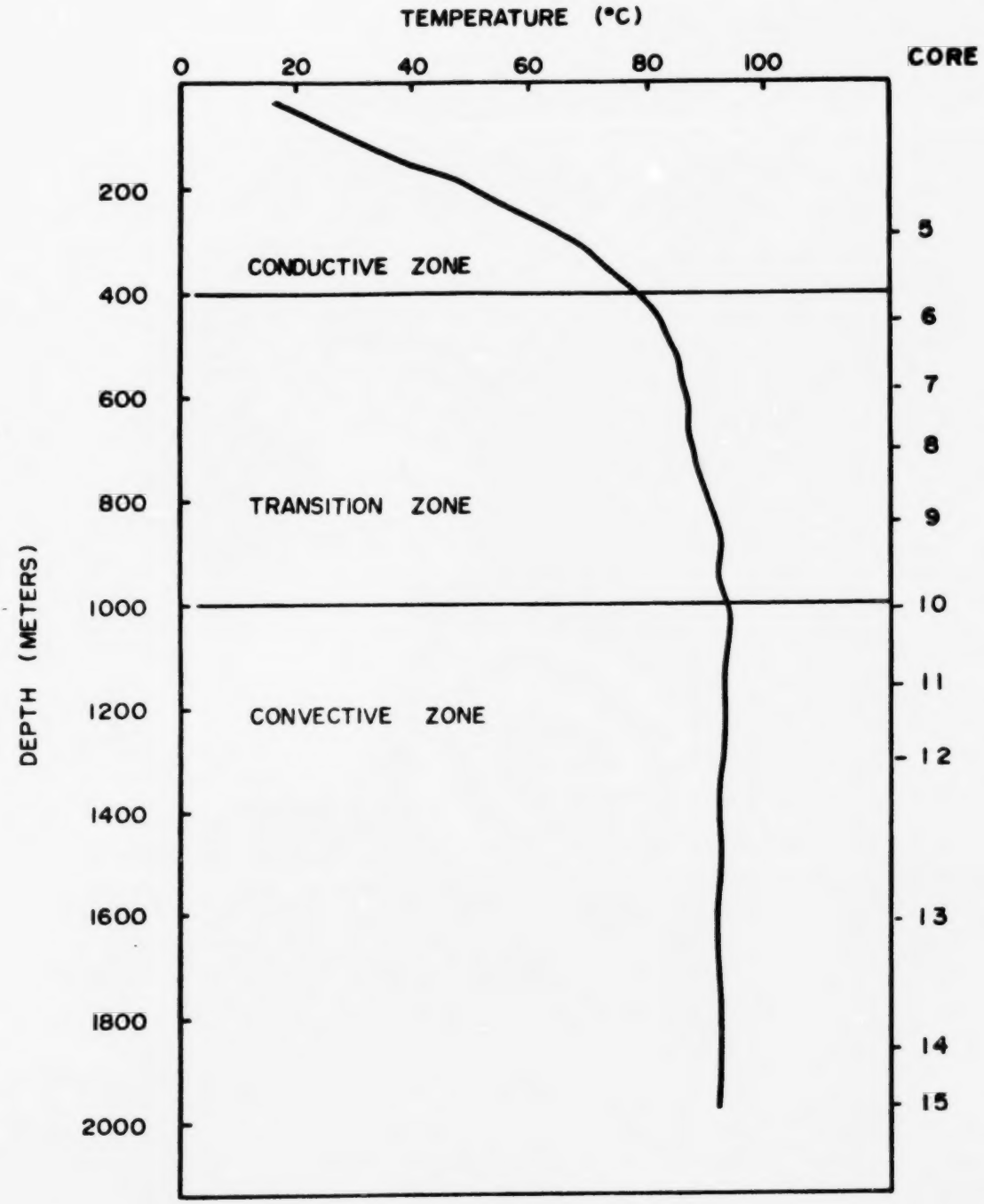

FIGURE 5 - TEMPERATURE VERSUS DEPTH IN THE DEEP GEOTHERMAL BOREHOLE[26], SHOWING LOCATIONS OF CORE SAMPLES.

The essential primary mineralogy of the Empire Creek Stock cores is relatively consistent in composition from Core 5 through Core 15 (see Figure 5 for core locations). Significant textural variations occur throughout the stock, but essential minerals consist dominantly of subequal amounts of quartz and alkali feldspar (orthoclase microperthite), with lesser amounts of plagioclase (approximately An_5) and around 5 percent biotite. Accessory primary minerals consist of fluorite, zircon, monazite, apatite, niobian rutile, topaz, muscovite, and Fe-Ti oxides. Primary rock textures are generally porphyritic, with an aphanitic groundmass in Cores 5 and 6, and more coarsely crystalline groundmass present in the intermediate cores. The deepest cores, although still containing K-feldspar megacrysts are coarsely crystalline and more equigranular. Groundmass textures and phenocryst abundance are variable throughout the well. Although the finest grained groundmass is found in the highest core, and the overall groundmass texture becomes coarser-grained with depth, some variations occur, such as between Core 7 and 8 where the groundmass of Core 8 is finer-grained than that of Core 7.

Complex grain boundary textures are present, particularly in the feldspars, but locally also in quartz grains, throughout the core. In the upper porphyries, "sieve" texture commonly occurs in the rims of K-feldspar grains, and less commonly in quartz grains. In the upper porphyries, feldspar phenocrysts often occur as glomerocrysts as well as individual grains.

Inclusions of quartz and plagioclase are common in K-feldspar phenocrysts and megacrysts throughout the length of the well. In the deeper cores, fine-grained intergrowths of plagioclase or quartz are common along K-feldspar grain boundaries. Groundmass feldspar is subhedral in the upper porphyries, becoming more anhedral and locally interstitial in the lower cores.

Quartz phenocrysts throughout the well are moderately to strongly resorbed and embayed. Groundmass quartz occurs in equant individual grains in Core 5, but becomes more anhedral and interstitial toward the bottom of the hole.

Plagioclase throughout the well is generally close to albite in composition and only exhibits a minor amount of zoning in the lowest cores. Plagioclase

crystals are smaller than K-feldspar throughout the well and are generally euhedral to subhedral, particularly where they occur as inclusions in K-feldspar. K-feldspar domains in microperthite have near end-member composition (Or 95-98). Plagioclase phases in microperthite have near end-member composition (Ab 92-96), but are slightly more calcic (An 5-7) than groundmass albite (Ab 97, An 2, Or 1).

Of particular interest was the optically spectacular color zonation (from dark red-brown cores through light blue-green rims) in biotite from Core 10. This zonation was investigated to determine its relation, if any, to hydrothermal processes. During hydrothermal alteration of granite, primary igneous biotite (Fe-rich) is commonly replaced by secondary Mg-rich biotite due to reaction with hydrothermal fluids[28]. Therefore, it was expected that the color zonation migh correlate with an outward increase in Mg/Fe of the biotite. However, the data indicates minimal radial variation in Mg/Fe, although a sharp outward decrease in Ti content is evident. The Ti zonation probably accounts for the color zonation[38] and is interpreted to be a primary igneous effect rather than a hydrothermal effect. Although inclusions of niobian rutile (TiO_2 phase) were noted in the brown cores of biotite grains, these are less abundant in the low-Ti rims where they would be expected as a product of hydrothermal reactions that might have replaced high-Ti biotite with low-Ti biotite. In Core 5, unzoned brown biotite has composition similar to that of biotite cores in Core 10. Secondary muscovite is Fe-rich.

Alteration and vein morphology and mineralogy varies throughout the well. Core 5 is characterized by the most variable and complex alteration, veining and mineralization. Alteration and vein minerals include quartz, K-feldspar (adularia), sericite, biotite, chlorite, montmorillonite, kaolinite, fluorite, calcite, anhydrite, pyrite, topaz and molybdenite. Veining consists of a complex stockwork of crosscutting veins from discontinuous or horsetailing quartz veins to intensely altered zones of biotite-sericite-quartz-pyrite. Zoned veins indicating multistage alteration and mineralization episodes are also present. Alteration envelopes may not be present around veins.

Alteration is generally less intense in samples from the rest of the cores. Feldspars are variably altered to sericite and/or kaolinite ± montmorillonite in the middle cores, with the strongest kaolinite alteration occurring in Core 12. Partial alteration of plagioclase and biotite to calcite ± chlorite is common in Core 13, and biotite in Core 15 is partially altered to bright green chlorite. Minor amounts of K-feldspar, biotite, chlorite, sericite and flourite are present in veins in some of the other cores, but the most prominent type of veining is quartz veining which occurs as cryptocrystalline to microcrystalline fracture filling of intensely fractured and/or sheared and brecciated wall rock. Veining ranges from passive fracture filling of shattered rock to brecciation and obvius displacement of rock and mineral fragments. Veining and/or brecciation were observed in Cores 13 and 15, but are present in all other cores.

Miarolitic cavities are common in Cores 13, 14 and 15 and are partially to completely filled with fluorite, calcite, muscovite or quartz. Where present in the upper cores they are generally filled with quartz or kaolinite.

In addition to petrographic analyses, standard whole rock chemical analyses were performed on four samples from various depths from the deep borehole. The analyses were performed by Barringer Magenta Ltd., Calgary and the results are presented in Table 2. Uranium and thorium abundances for selected samples are tabulated in Table 8.

2. Fracture and Alteration Mineralogy

X-ray diffractometry (XRD) and scanning-electron microscope (SEM) analyses were undertaken to determine the mineralogy of fractures and alterations in the core. This was felt to be important since this mineralogy is related directly to the hydrothermal convection which has occurred in the stock.

Qualitative analysis of alteration from Cores 8, 11, 12 and 15 by x-ray diffractometry (XRD) performed at the Argonne National Laboratory, Argonne, Illinois, indicates that the presence of a significant amount of kaolinite, with lesser but variable amounts of quartz, fluorite and albite, ± illite.

Table 2 - Chemical Analyses of ECS Rocks
(Values in % unless otherwise stated)

	SAMPLE NO.*			
	3	6	21	35
SiO_2	75.4	78.8	77.1	75.5
Al_2O_3	11.7	9.7	11.2	11.5
Fe_2O_3	1.46	2.42	2.00	2.11
CaO	0.55	0.93	0.92	0.70
MgO	0.18	0.19	0.05	0.16
TiO_2	0.053	0.050	0.069	0.172
MnO	0.027	0.040	0.049	0.046
Na_2O	3.7	<0.7	3.1	3.4
K_2O	4.0	2.3	4.7	4.2
P_2O_5	<0.3	<0.3	<0.3	<0.3
LOI	1.29	2.33	0.72	0.47
Ba(ppm)	60	80	120	130
F (ppm)	-	-	-	3080

* 3 is a porphyry rock from core 5.
6 is an altered biotite/sericite rock from core 5.
21 is from core 10.
35 is fresh granite from core 15.

Illite peaks are coincident with sericite, muscovite and biotite peaks, so a mineral identified as illite is probably sericite and/or biotite. A "chalcedonic" vein from one of the cores is composed primarily of alpha quartz with a minor amount of kaolinite.

A thin brown coating on fracture surfaces and kaolinite alteration in plagioclase grains in Core 12 was hand picked for XRD analysis, but only kaolinite (35 percent), illite (sericite - 24 percent, quartz - 26 percent and feldspar - 14 percent) were detected in significant amounts along with 1 percent calcite.

Cuttings samples were selected for x-ray diffractometry from within or as close as possible to significant fracture zones within the well as determined by geophysical log analysis, drilling reports, or high water flow. Some of the samples were hand-picked under a binocular microscope to separate possible alteration, vein or fracture-fill material. Results of bulk x-ray diffraction analysis of each cuttings sample as well as analysis of the clay fractions of the cuttings samples and/or the hand picked portion are summarized in Table 3. No minerals were detected which were not observed optically as well, although the wide range of secondary feldspar peaks could have masked peaks of minor minerals. The higher proportion of quartz in the bulk analysis of sample 1520/25 probably reflects the abundant quartz veining and increased silica in altered zones. The high illite content in the hand picked sample may represent preferential sampling of sericitic alteration. Only very minor amounts of montmorillonite were detected in the cuttings. Up to 4 percent kaolinite was detected in the bulk analyses of the cuttings samples, the highest value obtained in the deepest sample (2053 m); however, due to the possibility of peak enhancement by secondary feldspar peaks, this value may be too high. In comparison, the amount of kaolinite present in the glycolated clay fraction of the 2053 m sample is only 12 percent compared with 32 percent in sample 1804 m and 20 percent in the sample from 1169 m.

Fracture surfaces and porous zones from Core 12 samples were examined on a scanning electron microscope equipped with an x-ray energy spectrometer.

Table 3 - Results of XRD Analyses of Cutting Samples

BULK ANALYSIS

Depth (m)	Qtz	Plag	K-Feld	Koal	Ill	ML	Chl	Sm
463	46.0	29.0	23.0	Tr	2.0		Tr	
1169	37.0	36.0	25.0	Tr	2.0		Tr	
1349	36.0	39.0	24.0	Tr	1.0		--	
1804	34.0	36.0	26.0	2.0	2.0		--	
2051	30.0	35.0	30.0	1.0	1.0		2.0	
2053	31.0	34.0	26.0	4.0	2.0		2.0	

CLAY FRACTION

463	6.0	9.0	7.0	6.0	63.0	1.0	5.0	3.0
463	6.0	20.0	19.0	13.0	33.0	4.0	3.0	3.9
1169	13.0	21.0	17.0	18.0	28.0		3.0	tr
1169	6.0	15.0	14.0	20.0	38.0	2.6	3.9	1.0
1349	16.2	27.0	19.8	10.5	26.6	tr		tr
1804	9.6	28.1	15.7	32.1	14.5	--	--	--
2051	19.2	21.0	18.0	13.2	21.6		7.2	
2053	4.0	21.1	18.9	11.7	26.6	3.2	11.3	3.2

In addition to kaolinite, other secondary minerals identified included submicroscopic quartz crystals, calcite and anhydrite. Calcite and anhydrite were detected in only trace amounts, but minute quartz crystals have formed on fracture surfaces and within porosity in leached feldspars. No other fracture coating minerals are identified either visually or by elemental analysis during scanning electron microscopy.

3. Porosity and Permeability

Porosity, permeability and grain density measurements were performed and results for four core samples and one standard sample are summarized in Table 4.

Table 4. Porosity, Permeability and Density Data

	Porosity(%)	Permeability (milliDarcies)	Grain Density (Kg/m3)
Core 5	6.7	0.01	2729
Core 11	11.6	0.01	2682
Core 12	8.8	1.01	2678
Core 14	4.5	0.01	2636
Lac du Bonnet Granite	0.1	-	2630

The high porosity values in Cores 5, 11 and 12, in part reflect the abundance of clay alteration. The fabric of aggregates of clay minerals is highly microporous. The very high porosity values for Cores 11 and 12 also reflect the abundance of fractures and the microscopic voids along quartz veins. In addition, a certain amount of microporosity is present within altered feldspars, either due to direct leaching of feldspar or due to leaching or physical removal by water of alteration products. Microporosity within the fabric of aggregates of kaolinite booklets and platelets, and microporosity within leached feldspars was observed during SEM examination of Core 12 samples. Pore spaces in leached feldspars generally are controlled by cleavage direction and generally are less than 3 um in diameter.

Pore space within clay alteration in Core 14 is mainly composed of miarolitic cavities. Some fracturing and veining was observed in thin section of Core 14, and some porosity may be associated with this fracturing and veining, if it was present in the particular portion of the sample cut for analysis.

The permeability values for Cores 5, 11 and 14 were below the detection limits of the analysis technique, but a permeability of 1.01 millidarcies was measured for Core 12. This comparatively large value probably represents permeability along a fracture present in this sample rather than only through the micropores of feldspars and clays.

A sample of the Lac du Bonnet granite from eastern Manitoba was submitted with the Empire Creek stock cores for use as a check on the reliability of the methods employed for measuring porosity and density. The physical properties of the Lac du Bonnet granite have been thoroughly studied as part of the Canadian nuclear waste disposal program and yield a porosity of 0.24% and a density of 2640 kg/m^3, which are in good agreement with the values determined in this study for Lac du Bonnet granite (Table 4).

The Empire Creek Stock core samples have a large porosity which is much greater than values generally reported for granites.

4. Fluid Inclusions

Fluid inclusions form when fluid is either trapped along growth irregularities as the crystal grows or introduced along fractures after the crystal forms. The fluid is then isolated by the enclosing crystal. Assuming that the volume of the inclusion remains constant after it forms and the material within the inclusion remains isolated, cooling of the inclusion results in shrinkage of the fluid. This nucleates a vapour phase which is essentially a vacuum forming a two-phase (liquid vapour) inclusion. Upon reheating, the fluid within the inclusion will expand and eventually refill the inclusion with a single fluid phase. The temperature at which this occurs (the homogenization temperature) gives an indication of the temperature at which the fluid was trapped.

Vein quartz was sent to the University of Calgary for fluid inclusion analysis. Unfortunately, fluid inclusions within most of the microcrystalline to cryptocrystalline quartz veining in the lower cores are too small to analyze. Quartz veins are coarser grained in Core 5, and consequently, fluid inclusion size is within the resolution of the fluid inclusion microscope optics permitting the analysis of several samples. Although a few inclusions of suitable size were visible in thin sections of Core 10, only one measurement was possible.

The homogenization temperatures (T_h) of 66 inclusions in quartz veins were measured and are reported in Table 5. The inclusions were assumed to be primary if they were not located on obvious fracture surfaces. The majority of the inclusions are two-phase liquid and vapour. Two inclusions contained solids which appeared to be cubic halite crystals. These crystals, which probably grew from a NaCl saturated fluid contained within the inclusion, dissolved on heating to the homogenization temperature of the inclusion. There was no evidence for the presence of a CO_2 or CH_4 phase in the inclusions.

Table 5. Fluid Inclusion Data for Quartz Vein Samples

Sample No.	Core	No. Measurements	T_h (°C) (range)	T_h (°C) (average)
1b	5	9	224.6-376.1	329.3
1c	5	7	210.3-297.3	250.8
	5	5	198.0-228.3	211.2
2	5	31	195.0-357.5	269.3
3	5	4	301.6-321.1	309.0
		9	233.1-322.8	294.2
23	10	1	-	290.6

The T_h for the first five inclusions was measured twice in order to test the reproducibility of the data. The inclusions were generally reproducible to ± 2°C. After determining that the homogenization temperatures were very consistent from one heating run to the next, the remainder of the measurements were done only once. The homogenization temperatures measured are given in Table 5. Inclusions in the same vein which had similar temperatures tended to occur on the same plane in the same region of the crystal. T_h seems to increase from the base to the rim of the crystal in the direction of growth.

The homogenization temperatures of these two-phase inclusions give an indication of the temperature at which the host crystal grew. For Core 5, in which most of the measurements were made, the temperatures range from 195.0 to 376.1°C with the majority of the temperatures falling between 225 and 325°C. The large range of temperatures is interpreted as being caused by multiple generations of vein filling growing from fluids of varying temperatures. The temperatures in some cases appear to increase from the base to the rim of the quartz crystals in the direction of crystal growth, implying the flow of fluids of increasing temperatures through the open fractures in the rock. Only one homogenization temperature was measured in Core 10 due to the extremely small size of the inclusions and this value (290.6°C) is quite similar to those measured in Core 5.

5. Oxygen Isotopes

Oxygen isotope ratios were measured in quartz and feldspar separates from Cores 5, 12 and 15. The separates were derived from narrow (1-2 cm) sericite-biotite alteration zones adjacent to a molybdenite-bearing vein in Core 5, chalcedonic quartz from a vein in Core 9, and kaolinite replacing albite in Core 12. Oxygen was liberated from the samples for isotopic analysis by the BrF_5 method[39], and analyzed as CO_2 using a dual inlet-dual collector mass spectrometer. Data are reported in per mil ($^0/_{00}$) deviations from Standard Mean Ocean Water (SMOW):

$$\delta\,^{18}O = \left[\frac{(^{18}O/^{16}O)_{sample} - 1}{(^{18}O/^{16}O)_{SMOW}} \right] \times 1000$$

Analytical uncertainty (1 sigma) of the analyses is $0.14^{o}/_{oo}$. Data are given in Table 6. Unaltered granitic igneous rocks normally have ^{18}O in the range of +6 to $+10^{o}/_{oo}$, and exhibit quartz-alkali feldspar fractionations (ΔQ-F = QUARTZ - ALKALI FELDSPAR) of 1.0 to $1.5^{o}/_{oo}$[29]. Studies of rocks from fossil hydrothermal systems around granitic intrusions have demonstrated that whole rock ^{18}O values are substantially lowered, and ΔQ-F values significantly increased as a result of high temperature oxygen exchange between the rocks and circulating low ^{18}O meteroic groundwaters. Quartz-feldspar fractionations in these systems increase because the rate of oxygen exchange between felspar and and water is much greater than than between quartz and water[31], therefore, $\delta\,^{18}O_{QUARTZ}$ changes not at all or only slightly while $\delta\,^{18}O_{FELDSPAR}$ decreases by a significant amount.

Table 6. Oxygen Isotope Data for Mineral Separates from the Empire Creek Stock

CORE		^{18}O SMOW
5	Dark Green Alteration Zone	5.2
5	Pale Green Alteration Zone	3.1
5	Quartz	7.0
5	Alkali Feldspar	-0.6
9	Chalcedonic Quartz Vein	7.8
12	Quartz	9.5
12	Alkali Feldspar	6.4
12	Kaolinite Replacing Albite	2.4
15	Quartz	9.1
15	Alkali Feldspar	6.8

Data from the Empire Creek stock indicates that the rock of Core 5 probably experienced significant high-temperature oxygen exchange with low ^{18}O meteoric fluid, as evidenced by the fact that $\delta\,^{18}O_{QUARTZ}$ is lower than, and Δ Q-F is much larger than those of normal granites[29]. The analyses of the sericitic alteration zones adjacent to a molybdenite-bearing vein in Core 5 also indicate abnormally low $\delta\,^{18}O_{WHOLE\ ROCK}$ of 3.1 to 5.2.

The average homogenization temperature of 65 fluid inclusions in Core 5 quartz veins is 277°C (Table 2). Alkali feldspar in Core 5 would be in equilibrium with H_2O having $\delta\,^{18}O \approx -7^{o}/oo$ at 277°C[32]. Therefore, it is reasonable to assume that the observed depletion in ^{18}O in Core 5 occurred as a result of oxygen exchange with low ^{18}O water when these fluid inclusions were trapped. This presumably occurred at the time of late to postmagmatic molybdenite mineralization and associated sericitic alteration observed in Core 5, which is consistent with K-Ar data for sericite from Core 5 (next section).

Data for quartz and feldspar from Cores 12 and 15 show less evidence for significant oxygen exchange. Both quartz separates have normal ^{18}O values that are equal within anlytical error, and are thus nondiagnostic. Δ Q-F values are 3.1 and 2.3 for Cores 12 and 15 respectively, somewhat higher than the normal values of 1.0 to 1.5 given by Taylor[29]; these could be due to the late to postmagmatic alteration event that is most pronounced in Core 5. Alternatively, the present low-temperature water circulation could have been responsible for this modest lowering of $\delta\,^{18}O_{FELDSPAR}$ in Cores 12 and 15. Oxygen isotope data for water from the deep drill hole and surroundings are given by McSpadden et al.[8]. Drill hole water has $\delta\,^{18}O$ values -19.0 to -18.6, that are essentially identical to those of near-surface waters. A maximum $\delta\,^{18}O$ shift of $+0.5^{o}/oo$ may be inferred for one water sample collected from the 579m depth in the drill hole. Alkali feldspar equilibrium with drill hole water at 95°C would have $\delta\,^{18}O \approx -1^{o}/oo$, thus, prolonged contact of water and rock would result in ^{18}O depletion of feldspars. However, at 95°C, mm-size grains would require millions of years for significant oxygen exchange to occur[40]. An analysis of chalcedonic quartz from Core 9 ($\delta\,^{18}O$ = 7.8) suggests that this mineral may have formed under conditions similar

to those of the present warm hydrothermal system. Based on the quartz-water fractionation curve of Clayton et al.[33], a temperature of 62°C can be estimated for the deposition of the chalcedonic quartz vein in Core 9, assuming the present value of $\delta\,^{18}O_{WATER}$ (-19). In order to have been deposited at the current temperature of 95°C, this vein must have precipitated from water having $\delta\,^{18}O = -13$. Thus, if this vein is related to the present system either the temperature has increased ≈ 30°C, or the $\delta\,^{18}O_{WATER}$ has decreased by ≈ 5, since the vein formed. Alternatively, the vein could have precipitated at higher temperatures from water with higher $\delta\,^{18}O$ values (e.g. at 277°C water having $\delta\,^{18}O \approx 0$).

Kaolinite replacing albite in Core 12 has $\delta\,^{18}O = 2.4$. Assuming that the smectite-water curve of Yeh and Savin[34] is valid for kaolinite-water fractionation, a temperature of 46°C can be calculated assuming -19‰ water. Kaolinite forming in equilibrium with -19‰ water at 95°C would have $\delta\,^{18}O = -4.1$. A possible explanation for the apparently high ^{18}O value of the Core 12 kaolinite is that the water involved in the replacement reaction had undergone a a significant local upward shift in $\delta\,^{18}O$ (≈ 7‰) during reaction with relatively high ^{18}O albite.

6. Potassium - Argon Age Dating

Two samples of the Empire Creek stock, one from Core 5 and the other from Core 15, were submitted for conventional potassium-argon age determination by the Geochron Laboratories of Krueger Enterprises. A sericite mineral concentrate from the highly altered portion of Core 5 was separated and analyzed rather than the whole rock, in an attempt to date the time of hydrothermal quartz-sericite alteration. The Core 15 sample was fresh, pink, coarse-grained granite, and a potassium feldspar separate (orthoclase microperthite) was analysed from the sample to determine the age of emplacement and cooling of the deep portions of the Empire Creek Stock. The analytical results from the K-Ar age determinations are presented in Table 7. An age of 38.5 +/- 1.5 my was determined for the sericite concentrate from Core 5, and an age of 37.8 +/- 1.5 my was determined for the fresh orthoclase microperthite from Core 15. These ages are identical within analytical uncertainty, indicating

Table 7. Analytical Data for K-Ar Age Determination

Sample	^{40*}Ar(ppm)	^{40*}Ar/Total^{40}Ar	K(%)	^{40}K(ppm)	AGE(10^6yrs)
Core 5	.01497	.702	5.545	6.615	38.5 +/- 1.
Core 15	.02108	.771	7.967	9.505	37.8 +/- 1.

^{40*}Ar refers to radiogenic ^{40}Ar

that the sericitic alteration in Core 5 probably occurred near the time of emplacement of the stock, and temperatures have since remained below the K-Ar blocking temperature.

7. Uranium Disequilibrium Analyses

Seven samples from various depths in the boreholes were analyzed for uranium disequilibrium by Dr. M. Gascoyne, Atomic Energy of Canada Ltd. Powedered granite samples were fused and then uranium and thorium were seperated using solvent extraction and ion exchange resin methods. The separates were plated onto steel discs and analyzed using alpha spectrometry. The method has been described by Gascoyne and Larocque[35], and results are presented in Table 8. Uranium abundance in the samples range from 10 to 30 ppm, which is above averagee for granite.

The results given in Table 8 show that all of the $^{234}U/^{238}U$ activity ratios lie within one standard deviation of 1.00 (secular radioactive equilibrium). This means that neither ^{234}U nor ^{238}U has been selectively leached from the samples over the last one million years (approximately four half-lives of ^{234}U. Similarly, all $^{230}Th/^{234}U$ activity ratios lie within 3 standard deviations of 1.00, indicating that neither ^{230}Th nor ^{234}U has preferentially leached over approximately the past 350,000 years. In light of the relatively vigorous hydrothermal activity which has been observed, these results are somewaht unexpected.

Two interpretations are possible. The first is that the observed mineralogical alteration is not caused by present conditions, and is at least one million years old. The alternative, but less plausible, explanation is that alteration is occurring at the present time, but at a sufficiently slow rate to allow the uranium series isotope systematics to remain in equilibrium.

Table 8. Data from Uranium Disequilibrium Analyses

Sample No.	Depth(m)	U(ppm)	Th(ppm)	$^{234}U/^{238}U$*	$^{230}Th/^{234}U$*
1910/15	1910	10.0	39.1	0.98(0.04)	1.10(0.06)
1525/30	1525	14.8	32.5	1.01(0.04)	0.97(0.06)
3385/90	3385	10.9	32.1	0.97(0.04)	0.98(0.06)
6735/40	6735	10.7	+	1.02(0.04)	+
5-6	305	21.3	49.9	0.98(0.03)	1.00(0.04)
14-34	1836	17.7	46.6	0.95(0.03)	0.98(0.05)
12-30	1298	30.5	108	1.01(0.02)	1.11(0.05)

* Isotope activity ratios. Numbers in brackets represent one standard deviation.

+ Th data not available.

F. DISCUSSION/SYNTHESIS

1. Introduction

Any interpretation of the petrographic and specialized analysis data obtained from the Empire Creek stock (ECS) core samples must take into account the fact that only a total of 14.7 m of core from 11 cored intervals has been used to represent the 1776 m drilled through the Empire Creek stock. Cuttings samples, where available, were too fine grained to be of use in petrographic analysis.

2. Emplacement of the Empire Creek Stock

Analyses of the Empire Creek stock samples indicate that the stock is a composite intrusive body made up of a small number of genetically related and compositionally similar granite porphyry stocks and dikes, probably successive intrusive pulses from a common deep magma source. Due to lack of continuous core recovery, no intrusive contacts were observed, but textural variations, such as the finer grained groundmass in the porphyry of core 8 than in the porphyries of core 7 or core 9 indicate that several different intrusive bodies are present. Relative ages cannot be determined between the different bodies, however, without contact relationships. Mineralogy is similar throughout the core, but slight variations such as the strongly zoned biotite throughout the middle cores compared to the biotite in the lower cores, and the irregular distribution of minerals such as topaz, may be related to specific intrusive episodes.

The presence of biotite, muscovite, fluorite and locally topaz and calcite in relatively unaltered rock, as well as the miarolitic cavities, particularly in the lower cores, indicate a relatively high volatile content in the magmas.

Complex grain boundary and grain contact relationships, such as resorption and regrowth of quartz and feldspar grains, sieve texture in quartz, reaction rims of feldspars of different compositions between adjacent feldspar grains or around feldspar phenocrysts, and inclusions of embedded plagioclase or

quartz grains within potassium feldspar phenocrysts or megacrysts, all indicate that the various intrusions have undergone a complex crystallization and cooling history characterized by changing pressure, temperature and chemical conditions. Some of these conditions may have been related to venting at the surface during the eruption of the apparently contemporaneous Hope Creek rhyolitic volcanics.

3. Post-Magmatic Alteration

Alteration, fracturing and veining have affected most of the samples examined in some way. In the deepest core, alteration of biotite to chlorite, incipient clay or clay-carbonate alteration of feldspars, and some fluorite and muscovite in biotite sites are evidence of deuteric alteration by residual solutions and volatiles during late magmatic and post-magmatic stages of consolidation. Intense fracturing of rock and shattering of grains in the middle cores took place at least in part after complete consolidation, but healing of fractured grains by magmatic minerals, and discontinuity of fractures as they pass into less competent minerals suggests that some fracturing took place very early.

Cross-cutting relationships of veining and alteration and the variability of alteration in core 5 indicates a very complex series of physical, chemical and hydrologic conditions have affected the upper porphyries during consolidation and cooling of the magma. The alteration observed in the upper cores is characteristic of a post magmatic hydrothermal system, probably with a significant meteoric component.

Minerals such as fluorite, calcite, topaz and muscovite occur both as late magmatic or pneumatolitic primary minerals and as secondary minerals in vein fillings or alteration zones. Quartz is an ubiquitous secondary mineral, occurring as filling in very early, discontinuous fractures formed when the intrusive bodies behaved in a more plastic manner, as well as in veins and breccia zones.

The alteration, mineralization, veining and host rock of the Empire Creek porphyries are typical, in texture, composition and distribution of the porphyry copper/molybdenum deposits throughout western North and South America[36].

Porphyry molybdenum deposits are generally associated with granite porphyries intruded at relatively shallow depths, and are characterized by fracturing, vein stockworks, hydrothermal alteration, strong silicification and the presence of topaz and fluorite. Alteration types include potassic (characterized by potassium feldspar and secondary biotite), argillic (characterized by montmorillonite and/or kaolinite) and quartz-sericite (where the rock is so completely altered to quartz and sericite that primary rock texture is poorly preserved). Sample recovery is not good enough to determine the distribution of alteration types, but core 5 samples contain the most variety and most strongly developed alteration and veining of all the cores recovered.

The shallow depth of emplacement and multiple intrusive nature of the Empire Creek stock as well as the regional tectonic setting have resulted in the formation of an extensive system of fracturing and veining throughout the entire stock. Some of the fractures probably formed in response to intrusive forces during successive stages of porphyry intrusion. Cooling at shallow depths probably resulted in shrinkage fracturing within the porphyry bodies, and fluid pressures from a high volatile content and/or an influx of heated meteoric water probably also contributed to internal pressures which could have resulted in fracturing of the stock. Intense brecciation and shattering of the wall-rock evident in cores 11 and 12 may be a result of hydro-fracturing due to a build-up of fluid pressure. The ECS is in a tectonically active area, and major crustal adjustments taking place in the region during or after emplacement and cooling of the composite stock may also have contributed to the fracturing and brecciation over the last 38 million years.

4. Subsequent Alteration

The primary purpose of the investigation of the geology of the samples from the Marysville Deep Geothermal Well was to determine the relationship of the present-day low-temperature, geothermal system to alteration, veining and fracturing within the Empire Creek Stock. Petrographic examinations, K-Ar dating and fluid inclusion geothermometry indicate that the hydrothermal

alteration of the upper cores, at least, occurred during the post-magmatic phase of the cooling of the porphyry intrusions. Although abundant microporosity is present within clays in this upper zone, fractures are tightly sealed by silica or other secondary minerals.

In the deeper cores, some open fractures are apparent, altered feldspars (core 12) appear leached and plagioclase feldspars are strongly kaolinized. Microcrystals of quartz have formed on fracture surfaces, across leached and altered feldspars. These quartz crystals appear to have precipitated from circulating waters, and may have formed from waters of the present convective geothermal system that is nearly saturated with quartz.

Figure 6 shows water compositions from the Marysville deep drill hole [27] plotted on an activity ratio diagram for the system H_2O-Al_2O_3-K_2O-Na_2O-SiO_2-HCl at quartz saturation at 100°C from Helgeson et al.[37]. This diagram represents the stability relations of the alkali feldspars, muscovite (sericite), Na-montmorillonite and kaolinite under the approximate conditions encountered in the drill hole, as a function of fluid composition. At pH values below 7.5, Marysville drill hole water would be in equilibrium with kaolinite at 100°C. This suggests that the ubiquitous kaolinite alteration of albite in the drill core could be a consequence of prolonged interaction with the present warm convecting water, if the pH of this water is less than 7.5. Field pH measurements of Marysville drill hole samples were generally in the range 7.5 - 8.0[27]. However, pH values of deep thermal water samples commonly increase after collection and cooling due to loss of dissolved CO_2, decreased dissociation of water, and other effects, thus, the actual pH of water circulating throught the Empire Creek Stock is probably somewhat less than that measured.

Oxygen isotope data for kaolinite from core 12 and cryptocrystalline quartz, vein material from core 9 are consistent with formation under present geothermal conditions. Unfortunately it has not been possible to date this material. There is no reason, however, that the Empire Creek stock could not have undergone more than one period of geothermal convection during the past 38 million years. A fracture system has been present since the emplacement and

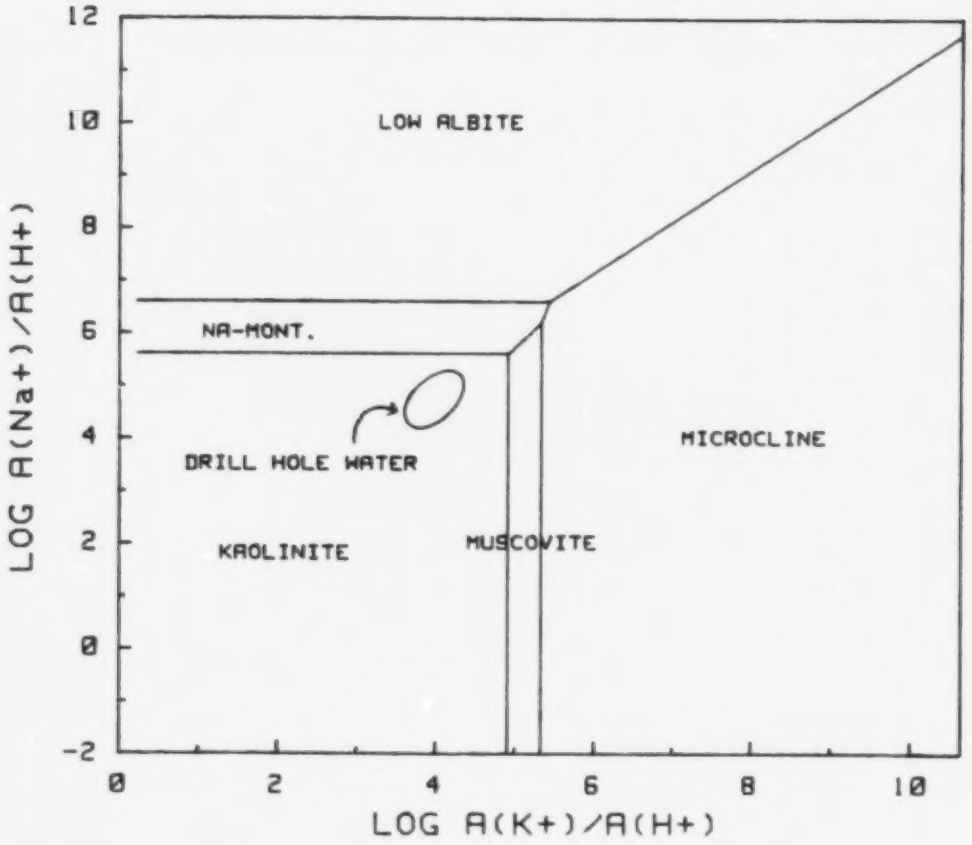

FIGURE 6 - THE SYSTEM HCl - H_2O - Al_2O_3 - K_2O - Na_2O - SiO_2 AT 100°C SHOWING FIELD OF DEEP DRILL HOLE WATER COMPOSITION (AFTER HELGESON[37]).

cooling of the intrusive complex, and the region has been tectonically active. None of the alteration, veining or fracturing throughout the core is inconsistent with processes which would have occured during initial consolidation and cooling of a volatile-rich magma at shallow depths where interaction with meteoric water would be a natural occurrence.

The uranium disequilibrium analyses show that even at the deeper borehole levels the uranium series isotopes are in equilibrium. This fact implies that the observed rock alteration has not occurred in the past 1 million years. Together with the K-Ar dating data these analyses suggest that the alteration was formed during the late-emplacement and post-emplacement phases of the stock. It is rather surprising that no significant uranium disequilibrium is present in light of the observed, relatively vigorous, hydrothermal convection in the stock at approximately 75°C. Uranium disequilibrium is common in surface and near-surface rocks and, hence, some physical and chemical conditions must be sufficiently different at depth within the Empire Creek Stock to prevent uranium and thorium isotope fractionation in spite of the high measured porosity of the rocks and the hydrothermal circulation. This topic clearly warrants further research since it implies that it may be very difficult to remove transuranic elements from a nuclear waste repository and transport them to the biosphere via groundwater circulation. Alternative hypotheses are available. For example, it is possible that the groundwater convection in the Empire Creek Stock has been initiated very recently and the uranium series has not yet gone into measurable disequilibrium. However, alternative hypotheses such as this are not very plausible.

5. Summary

As a natural analogue to a nuclear waste respository, the Empire Creek stock is a dichotomy. On the one hand, it provides a vivid example of how long term heat can result in very porous and permeable conditions in igneous intrusives and can cause vigorous, convective, ground-water motion. On the other hand, because of a complex intrusive, fracturing, veining and alteration history and the location in a tectonically active area, the Empire Creek stock is clearly not typical of plutons in the Canadian Shield. Because of this its direct usefulness as a suitable natural analogue for a nuclear waste repository in

granitic rock is limited. The stock was highly fractured and altered before the inception of the present geothermal system, so that the circulating waters are not interacting with fresh rock on fresh fracture surfaces as might be expected in a carefully chosen nuclear waste site. Rather they are interacting with variably altered rock on fracture surfaces which may already be coated by silica or other minerals from previous fracture-filling events. If fractures were to form in rocks sealed by earlier vein-filling, they would most likely form along old zones of weakness. Many veins and fractures in the Empire Creek stock samples show evidence of renewed activity along healed fractures.

Nevertheless, useful information is available from this study. Examination of core 12 indicates that porosity within altered zones can be much greater than has been recorded in the literature for granitic rocks. Circulation of a large amount of water through fractures in already altered rock could result in the leaching or physical removal of unstable or loosely packed, fine clays, increasing porosity within the altered zone. Scanning electron microscope examination of feldspars on fracture surfaces revealed corroded kaolinite crystals suggesting leaching by circulating fluids, and microporosity within fresh feldspar where either the mineral had been selectively leached or an alteration product had been selectively leached or physically washed away.

Since no samples have been extracted from the major fracture zones where the main convective circulation is taking place, it is not possible to say if minerals, other than quartz, are currently being deposited. Alteration of plagioclase feldspar to kaolinite might be taking place, but this remains to be confirmed.

It is not clear whether the recent, mild hydrothermal activity has been responsible for opening the deeper fractures or not. Certainly evidence from elsewhere suggests that open fractures are an unstable condition and that they will reseal eventually. Thus, it seems that the present mild, hydrothermal system has, at least in part, contributed to the unsealing of the preexisting vein-filled fractures and for the creation of the unusually high matrix porosity in the rock mass.

However, the significance of even a fairly open fracture system is not clear, since the uranium disequilibrium analyses indicate (rather surprisingly) that deep repository rock conditions inhibit movement of transuranic elements. No analyses were performed which provided evidence regarding fission product movement.

Regardless of the interpretations which may be placed on the preceding data, it is clear that the effects of long term heat on a granite/groundwater system are very complex. Natural analogues provide a very useful tool for understanding the phenomena that would be expected around a repository containing spent fuel.

6. Recommendations

As long as there is realistic consideration being given to the disposal of spent fuel either in conjunction with, or separate from, reprocessed waste, there is a requirement to understand the long-term effects of heat on rock and groundwater. It is recommended that the study of natural analogues such as the Empire Creek Stock form an integral part of any investigations to understand these long-term, complex effects. Section D describes a number of geothermal areas in western North America which might provide useful sites for analogue studies It is recommended that the dry hot rock geothermal project in New Mexico be reviewed from a nuclear waste disposal perspective.

There is a considerable amount of information still to be gleaned from the Empire Creek Stock. Some specific studies which could be performed are listed below:

- Fission track annealing studies of apatite might determine the age of the present, mild geothermal activity.
- The $^{40}Ar/^{39}Ar$ step-heating, age dating technique would be an excellent method of determining the thermal history of the minerals in the Empire Creek Stock.
- A study of the geochemistry and structure of the metasediments which overlie the Empire Creek Stock is recommended to understand why groundwater convection does not occur in these strata, but does in the Empire Creek Stock.

- A borehole with complete core recovery would allow sampling of groundwater, studies of permeable fracture zones and the study of many more relevant problems.

- The adjacent Marysville stock appears to be quite different than the Empire Creek stock in structural, thermal and hydrologic character. It would be very useful to quantify these differences and to understand why they occur. Such a study would greatly assist repository site selection, as well as performance assessment.

G. REFERENCES

1. M. Eisenbud, K. Krauskopf, E.D. Franca, W. Lei, R. Ballad and P. Linsalata, Natural Analogues for the Transuranic Actinide Elements: An Investigation in Mina Gerais, Brazil, Environ. Geol. Water Sci., 6, 1-10, 1984.

2. W.A. Elders and L.H. Cohen, The Salton Sea Geothermal Field, California, as a Near-Field Natural Analog of a Radioactive Waste Repository in Salt, BMI/ONWI-513, prepared for Office of Nuclear Waste Isolation, battelle Memorial Institute, Columbus, OH. 1983.

3. Acres Consulting Services Ltd., RE/SPEC Inc., Dilworth, Secord and Meagher and Associates, Atomic Energy of Canada Ltd., and W.L. Wardrop and Associates Ltd., A Disposal Centre for Irradiated Nuclear Fuel: Conceptual Design Study, Atomic Energy of Canada Ltd., AECL-6415, 1980.

4. S.A. Mayman, R.G. Charlword and J.L. Ratigan, Long-Term Thermal Response of a CANDU Fuel Disposal Vault, Atomic Energy of Canada Ltd., TR-134, 1980.

5. D.D. Blackwell, Heat Determination in the Northwestern United States, Geophys. Res., 74, 992-1007, 1969.

6. W.R. McSpadden, et al., The Marysville Montana Geothermal Project First Annual Report, Part 1, prepared for the National Science Foundation, 1974.

7. D.D. Blackwell, et al., Geological and Geophysical Exploration at Marysville Geothermal Area: 1973 Results, with a section on Contemporary Seismicity in the Helena Montana Region, prepared for the National Science Foundation, 1974.

8. W.R. McSpadden, et al., The Marysville Montana Geothermal Project, Prepared for the National Science Foundation, 1975.

9. H.Y. Tammemagi, G.E. Grisak and D.K. Parrish, A Case History of the Marysville Geothermal Anomaly from a Nuclear Waste Disposal Perspective, Atomic Energy Control Board, INFO-0092, 1983.

10. A.H. Lachenbruch and J.H. Sass, Heat Flow in the United States and the Thermal Regime of the Crust, in the Earth's Crust, It's Natural Physical properties, ed. J.D. Heacock, American Geophysical Union, Monograph 20, 1977.

11. P.A. Rona and R.P. Lowell (eds.), Sea Floor Spreading Centres: Hydrothermal Systems, Benchmark Papers in Geology/56, Hutchinson and Koss Inc., Stroudsberg, Penn., 1980.

12. R.P. Lowell, Circulation in Fractures, Hot Springs, and Convective Heat Transport on Mid-Ocean Ridge Crests, in Ref. 11, 26-40, 1980.

13. G. Herget, Regional Stresses in the Canadian Shield, in Underground Rock Engineering, (Proceedings of the Thirteenth Canadian Rock Mechanics Symposium, Toronto, May 28-29, 1980). Special Volume 22, Canadian Institute of Mining, Montreal, 1980.

14. L.J.P. Muffler, (ed.), Assessment of Geothermal Resources of the USA-1978. Geol. Survey. Circ. U.S., 790, 1979.

15. C.R. Bacon and W.A. Duffield (eds.), Coso Geothermal Area, Special Issue of Jour. Geophys. Res., 85, B5, 1980.

16. S.H. Ward, et al., A Summary of the Geology, Geochemistry, and Geophysics of the Roosevelt Hot Springs Thermal Area, Utah, Geophysics, 43, 1515-1542, 1978.

17. D.E. White, R.O. Fournier, L.J.P. Muffler and A.H. Truesdell, Physical Results of Research Drilling in the Thermal Areas of Yellowstone National Park, Wyoming, U.S. Geological Survey Professional Paper, 892, 1975.

18. M. Nathenson, T.C. Urban, W.H. Diment and N.L. Nehring, Temperatures, Heat Flow and Water Chemistry from Drill Holes in the Raft River Geothermal System, Cassia County, Idaho, U.S. Geological Survey Open-File Report 80-2001, 30, 1980.

19. P.R.L. Browne and W.A. Elders, Hydrothermal Alteration of Diabase, Heber-Geothermal Field, Imperial Valley, California, Geol. Soc. America, Abstracts with Programs, 8, 793, 1976.

20. H.D. Murphy, J.W. Tester, C.O. Grigsby and R.M. Potter, Energy Extraction from Fractured Geothermal Reservoirs in Low-Permeability Crystalline Rocks, Jour. Geophys. Res., 86, B8, 7045-7158, 1981.

21. J.G. Souther, Geothermal Potential of Western Canada, Proc. 2nd U.N. Symposium on Development and Use of Geothermal Resources, 1, 259-267, 1975.

22. J.F. Lewis and A.M. Jessop, Heat Flow in the Garibaldi Volcanic Belt, A Possible Canadian Geothermal Energy Resource Area, Canadian Jour. Earth Sci., 18, 366-375, 1981.

23. G.D. Robinson, M.R. Klepper and J.D. Obradovich, Overlapping Plutonism, Volcanism and Tectonism in the Boulder Batholith Region, Western Montana, in Studies in Volcanology, R.R. Coats, R.L. Hay and C.A. Anderson, eds., Geol. Soc. Am. Mem. 116, 557-576, 1968.

24. R.A. Friedline, R.B. Smith and D.D. Blackwell, Seismicity and Contemporary Tectonics of the Helena, Montana Area, Bulletin of the Seismological Society of America, 66, 81-95.

25. H.R. Baadsgaard, R.E. Rolinsee and J. Lipson, Potassium-Argon Dates of Biotite from Cordilleran Granites, Bull. Geol. Soc. Amer., 72, 689-702, 1961.

26. D.D. Blackwell, M.J. Holdaway, P. Morgan, D. Petefish, T. Rape, J.L. Steele, D. Thorstenson and A.F. Waibel, Results and Analyses of Exploration and Deep Drilling at Marysville Geothermal Area, in McSpadden, W.R., ed., the Marysville Montana Geothermal Project, National Science Foundation Research Report NSF-RA-N-75-320, 1975.

27. W.R. McSpadden, Temperature and Water Measurements in the Geothermal Well at Marysville, Montana, by Battelle Pacific Northwest Laboratories for the U.S.G.S. Contract No. USGS 14-08-0001-15177, 1977.

28. R. Beane, Biotite Stability in the Porphyry Copper Environment, Economic Geology, 69, 241-256, 1974.

29. H.P. Taylor, The Oxygen Isotope Geochemistry of Igneous Rocks, Contrib. Mineral. Petrol, 19, 1-71, 1968.

30. R.E. Criss and H.P. Taylor, Jr., An $^{18}O/^{16}O$ and D/H Study of Tertiary Hydrothermal Systems in the Southern Half of the Idaho Batholith: Geological Society of America Bulletin, 94, 640-663, 1983.

31. B.J. Giletti and R.A. Yund, Oxygen Diffusion in Quartz. Journal of Geophysical Research, 89, 4039-4046, 1984.

32. J.R. O'Neil and H.P. Taylor, Jr., The Oxygen Isotope and Cation Exchange Chemistry of Feldspars: American Mineralogist, 52, 1414-1437, 1967.

33. R.N. Clayton, J.R. O'Neil and T.K. Mayeda, Oxygen Isotope Exchange between Quartz and Water. J. Geophys. Res., 77, 3057-3067, 1972.

34. H.W. Yeh and S.M. Savin, The Mechanism of Burial Metamorphism of Argillaceous Sediments, 3. Oxygen Isotopic Evidence. Geol. Soc. Am. Bull., 88, 1321-1330, 1977.

35. M. Gascoyne and J.P.A. Larocque, A Rapid Method of Extraction of Uranium and Thorium from Granite for Alpha Spectrometry, Nuclear Instrumentation and Methods in Physics Research, 223, 250-252, 1984.

36. Open University, Porphyry Copper Case Study, 5333 PC, The Open University Press, Milton Keynes, UK, 1976.

37. H.C. Helgeson, T.H. Brown and R.H. Leeper, Handbook of Theoretical Activity Diagrams depicting Chemical Equilibria in Geological Systems Involving an Aqueous Phase at One Atm. and 0° to 300°C. Freeman, Cooper and Co., San Francisco, 253, 1969.

38. W. Deer, R. Howie and J. Zussman, An Introduction to the Rock-Forming Minerals, Longman, London, 1966.

39. R.N. Clayton and T.K. Mayeda, The use of Bromine Pentafluorite in the Extraction of Oxygen from Oxides and Silicates for Isotopic Analysis: Geochimica et Cosmochimica Acta, 27, 43-52, 1963.

40. B.J. Giletti, M.P. Semet and R.A. Yund, Studies in Diffusion-III. Oxygen in Feldspars: an Ion Microprobe Determination. Geochemica et Cosmochimica Acta, 42, 45-57, 1978.

H. ACKNOWLEDGMENTS

The authors are greatly indebted to the Atomic Energy Control Board of Canada who provided the financial support for this work, and J.L. Wallach, the Scientific Authority, for his many stimulating discussions and encouragement. The contributions of the following individuals has greatly benefitted this study: Dr. D.D. Blackwell (Southern Methodist University) provided the core and cutting samples. Mr. Al Waibel (Columbia Geoscience) loaned a number of thin sections and ideas to this investigation. Dr. M. Gascoyne (Atomic Energy of Canada Ltd.) performed the uranium disequilibrium analyses and provided considerable assistance in interpretation of the data. Prof. Muehlenbachs (University of Alberta) provided oxygen isotope data. Mr. B. Tani (Argonne National Laboratory) performed X-ray diffraction identification of a number of samples.

We are particularly indebted to Dr. N.C. Sturchio, Argonne National Laboratory, who not only assisted with a number of the analyses, but also made valuable contributions to the interpretation of the data.

APPENDIX A

DETAILED BOREHOLE LITHOLOGY

Core Five (303.9-306 m)

Core 5 consists of variably altered, mineralized and veined quartz monzonite to granite porphyry. The least altered porphyry ranges from light grey to pinkish grey with approximately 30 percent phenocrysts of quartz, K-feldspar, plagioclase and biotite enclosed in a fine grained groundmass of quartz, feldspar and biotite. The porphyry is cut by a complex system of veins and veinlets ranging from <1 mm discontinuous quartz veinlets with no alteration envelopes to more continuous veins with more complex mineralogy and alteration envelopes. Vein morphology and mineralogy and associated alteration are quite variable. Where porphyry appears to be relatively fresh, alteration visible in hand specimen consists of a local increase in pink K-feldspar, and alteration of the cores of plagioclase phenocrysts to montmorillonite and/or other clay minerals. Minor amounts of pyrite and lesser amounts of molybdenite are present along some veins and veinlets and to a lesser extent disseminated throughout the samples. Strong sericitization or sericitization and biotization has affected the rock along some veins, where the country rock has been intensely altered to a dark green quartz-sericite-biotite rock with the obliteration of much of the primary porphyry texture.

In the least altered porphyry where primary texture is relatively well preserved, equant quartz phenocrysts are resorbed and embayed, and crystal faces are poorly preserved. Quartz phenocrysts often contain inclusions of biotite or feldspar. Maximum quartz phenocryst grain-size inhand specimen is about 1.0 cm, but in thin section, average quartz phenocryst size is 0.4 to 0.6 cm.

In thin section, many of the orthoclase microperthite phenocrysts visible in hand specimen are actually glomerocrysts of orthoclase or orthoclase and

albite. Albite crystals are often completely included within orthoclase phenocrysts. Orthoclase less commonly contains biotite inclusions.

Outer rims of orthoclase in this porphyry are characterized by sieve texture of quartz inclusions. Some grains show sieve texture throughout, but these grains may represent sections through grain rims.

Most plagioclase (albite) is present as glomerocrysts. Some plagioclase appears to be partially replaced by K-feldspar.

Biotite is pleochroic dark green or green-brown to pale yellow-green where fresh. It is variably altered to an aggregate of carbonate, sericite, sphene and opaques (pyrite?).

The groundmass is made up dominantly of K-feldspar and quartz, with K-feldspar slightly more abundant than quartz. Groundmass quartz consists of subhedral to rounded equant grains 0.1 to 0.4 mm in diameter and averaging about 0.15 mm. Commonly groundmass quartz occurs as discrete grains surrounded by orthoclase grains or in contact only with one or two adjacent quartz grains. Groundmass K-feldspar is perthitic and is generally slightly coarser-grained than groundmass quartz. Incipient sericitization is evident both in groundmass and phenocrysts even in the least altered sample of Core 5. Sericite alteration occurs along cleavages of feldspars, along grain contacts and along fractures, as well as in altered biotite. In more altered samples, sericite veins crosscut rock fabric with pervasive sericitization decreasing on either side of the veins.

Fluorite, calcite, sphene and leucoxene are associated with the sericite veins. In more heavily veined and altered rock, vein mineralogy ranges from simple fine-grained quartz or quartz and pyrite to banded quartz-adularia-fluorite-carbonate veins. Most intensely altered rock (dark green altered zone in hand specimen) consists mainly of quartz, sericite and green secondary biotite with lesser amounts of fluorite, carbonate and pyrite. Adjacent to the dark green zone containing secondary biotite is quartz-sericite rock in which all primary

minerals except quartz are altered to sericite and quartz, with primary quartz grains showing evidence of secondary overgrowths. Previously sharp quartz grain boundaries are irregular and intergrown with sericite. Minor amounts of fluorite and pyrite are also present in the quartz-sericite rock. Trace amounts of hematite, leucoxene, sphene and topaz ar present in the altered rock.

Core Six (464.5-466.3 m)

Core 6 consists of pinkish grey granite or monzogranite porphyry with approximately 15 percent K-feldspar, 15 percent quartz, 7-10 percent plagioclase and 3 percent biotite phenocrysts in an aphanitic groundmass of quartz, feldspar and biotite. Potassium feldspar phenocrysts range up to 1.7 cm in diameter and are pink in color, giving the rock an overall pinkish color. Plagioclase crystals occur separately or as inclusions or intergrowths within larger potassium feldspar phenocrysts. Plagioclase phenocrysts are generally smaller than K-feldspar, rarely exceeding 1.5 cm in diameter.

Cores of plagioclase are moderately to strongly altered to chalky white or buff kaolinite. Quartz phenocrysts are euhedral to rounded and locally embayed. Biotite inclusions are common in the quartz. Biotite is black to greenish black with some associated pyrite. Core 6 is cut by horizontal to 65° thin (0.2 mm to 5 mm) dark-gray quartz veins which often are banded parallel to the wall rock. Width is variable along some veins, with thicker zones containing unaltered fragments of wall rock or mineral grains. Phenocrysts adjacent to quartz veins may be shattered with fractures infilled by vein quartz. A minor amount of pyrite is present in the veins. No obvious alteration halo is associated with the dark grey quartz veins. Discontinuous veins splay or "horsetail" into several hairlike interconnecting branches.

In thin section, Core 6 is generally less altered than Core 5. As in the Core 5 porphyry, feldspar commonly occurs in large glomerocrysts of orthoclase microperthite, orthoclase microperthite and albite, or albite. Both feldspars and quartz phenocrysts are resorbed and incipient sieve texture is evident

around rims of both K-feldspar (mainly quartz inclusions) and quartz (mainly feldspar with some biotite inclusions.

Plagioclase cores are moderately to strongly altered to kaolinite with lesser amounts of motmorillonite, and also are partially replaced or rimmed by K-feldspar.

Biotite is green or brown-green pleochroic to pale yellow or yellow-green. Dark brown pleochroic haloes are common around zircon inclusions within the biotite. The biotite is also moderately zoned with a dark green core and a pale blue-green to colorless rim.

The groundmass quartz in Core 6 is more variable in size and shape than the groundmass quartz in Core 5. In this core, groundmass quartz is commonly irregular in shape rather than equant and grain size averages 0.175 to 0.2 mm. Groundmass K-feldspar is generally coarser-grained than groundmass quartz and is subhedral to anhedral. Minor amounts of groundmass plagioclase are generally subhedral.

Accessory minerals include fluorite, which occurs in association with biotite and interstitially, and sieve-textured topaz.

Veining in Core 6 mainly consists of horsetailing and cross-cutting cryptocrystalline quartz veins with sharp contacts which locally contain sulfides and broken mineral and wall rock fragments. No wall rock alteration or alteration of included fragments has taken place along the cryptocrystalline veins. A less common vein type consists of more coarsely crystalline (but finer-grained than groundmass quartz), quartz, fluorite and pyrite. Biotite adjacent to this vein type is slightly more altered (to sericite and/or chlorite) than biotite throughout the rest of the rock. Round to oblong voids up to 0.6 mm but generally less than 0.2 mm are present in the cryptocrystalline quartz filled veins, but voids are not interconnected.

Core 7 (590.1-593.3 m)

Core 7 is a light greenish-grey granite porphyry containing up to 40 percent phenocrysts of quartz, potassium feldspar, plagioclase and biotite. Quartz phenocrysts are equant and range up to 0.9 cm in diameter. Potassium feldspar phenocrysts are milky white with a maximum grain size of 1.4 cm. Plagioclase is altered to greenish-buff clay minerals, and commonly occurs as inclusions in potassium feldspar. Fresh biotite is dark greenish black, but much of the biotite is altered to buff-colored clay minerals.

The core is cut by buff-grey "chalcedonic quartz" veins up to 4 mm wide but generally much thinner.

In thin section, Core 7 appears to have more abundant quartz and feldspar phenocrysts and glomerocrysts than the porphyries of Cores 5 and 6. Groundmass is coarser-grained than that of Cores 5 and 6, with quartz grains averaging about 0.4 mm. K-feldspar is perthitic and turbid due to submicroscopic clay alteration. Orthoclase commonly contains euhedral plagioclase inclusions.

Cores of plagioclase phenocrysts and inclusions are altered to kaolinite with trace amounts of montmorillonite and/or sericite orthoclase. Quartz phenocrysts are strongly resorbed and embayed. Biotite inclusions are common in quartz phenocrysts. Biotite is dark green, brown-green or blue-green pleochroic to pale yellow-green, green or colorless. Biotites are zoned from dark green or brown-green cores to light blue-green or colorless rims. Dark brown pleochroic haloes have formed around zircon inclusions within the biotite. Biotite is locally altered to kaolinite and/or chlorite. Accessory fluorite is commonly associated with the biotite, but also may occur interstitially.

The Core 7 porphyry is characterized by euhedral crystal faces of quartz and feldspar. These cavities are generally filled with kaolinite, kaolinite and microcrystalline quartz or microcrystalline quartz only. Rarely, open cavities partially lined by quartz are present.

The core is cut by cryptocrystalline quartz veins which contain sparse mineral and rock fragments derived from the adjacent wall rock. Interstitial to cryptocrystalline quartz in the larger veins is a high relief low to moderately birefringent mineral which may be a clay, probably chlorite. Along the wall rock contact of the largest vein in thin section, an irregular yellow-green band probably consisting of abundant chlorite with the quartz indicates the vein has undergone more than one episode of fracturing and rehealing as there are places where the chloritic (?) band has been cut off by the later cryptocrystalline quartz vein. Fluorite is associated with the earlier chloritic vein-filling phase.

Core 8 (699.5-710.0 m)

Core 8 is a light grey crowded porphyry with 50 to 60 percent phenocrysts which consist of 30 to 40 percent quartz grains up to 8 mm and milky white to pale pink potassium phenocrysts up to 1.2 cm long; 15 percent white plagioclase with cores locally altered to a green-buff aggregate of clay minerals; and 5 percent green-black fresh biotite and altered biotite crystals and crystal aggregates. The aphanitic groundmass is finer grained than the groundmass of Core 7.

The core is characterized by 75° to vertical horsetailing 0.2 mm to 1 mm quartz veining and silicified microbreccias of locally derived rock and mineral fragments. Wall rock between quartz veins is fractured and healed by silica. Local void spaces are present along quartz veins but are poorly interconnected. No alteration haloes are associated with quartz veining.

The Core 8 porphyry is similar in composition and texture to the Core 6 porphyry with the exception that quartz phenocrysts and feldspar phenocrysts and glomerocrysts are more abundant. Groundmass texture and grain size is similar to Core 6 groundmass and finer grained than Core 7 groundmass. Large quartz phenocrysts are mildly to strongly resorbed and embayed, but some grains retain their original euhedral outline. Feldspars show evidence of resorption and recrystallization. Some K-feldspar and plagioclase grains are rimmed by K-feldspar, and some plagioclase grains appear to be partially replaced by K-feldspar. Reaction rims around feldspars are marked by quartz inclusions, and some grains contain more than one inclusion-bearing zone.

Biotite is zoned, and generally lighter green in the center of grains than in the higher cores, but this may be due in part to the orientation of grains in thin section. Biotite is sparse in the available thin sections. Dark brown pleochroic haloes are present around zircon inclusions. Some biotite grains are partially altered to kaolinite and chlorite.

A 0.4 mm cryptocrystalline quartz vein cutting through one thin section has sharp contacts with the country rock. No alteration zone appears to be related to the vein, and no inclusions are preseent. Discontinuous parallel hairline fractures are also filled with cryptocrystalline quartz. Round to oblong voids are present along the main vein but are poorly interconnected.

Core 9 (848.0-849.2 m)

Core 9 is a pale grey to greenish grey granite porphyry containing phenocrysts of quartz (1.3 mm), orthoclase microperthite (1.4 cm), plagioclase (0.7 cm) and biotite (0.6 cm) in a fine-grained groundmass. Grain boundaries of quartz phenocrysts are irregular. Feldspars are partially altered, with orthoclase a chalky white, and plagioclase greenish grey. A 0.5 cm buff-colored quartz vein cuts core at an angle of 70 - 80°. The vein wall is lined by chlorite with a chloritic alteration zone extending 0.2 to 0.5 cm into the wall rock from the fracture surface. Pyrite is associated with the chlorite on fracture surfaces and in the chloritized wall rock. Some brecciation has taken place in the chlorite-quartz veins.

In thin section, the groundmass of Core 9 is coarser grained than the groundmass of Cores 8 and 7. Average groundmass quartz grain size is about 0.8 mm. As in the other cores, orthoclase microperthite megacrysts often enclose euhedral quartz or plagioclase feldspar grains. Quartz phenocrysts (to 1 cm in thin section) are resorbed and also contain inclusions of plagioclase and other quartz grains. Biotite is zoned from green cores to clear rims.

Orthoclase and plagioclase feldspars and primary biotite are moderately to strongly altered to sericite. Biotite is also partially altered to a fine-grained pleochroic green mica, probably secondary biotite or a mixture of biotite and chlorite.

Core 9 has been cut by multiple stages of veining. A chlorite-biotite vein is cut by a K-feldspar vein which has been sheared by later movement along the vein. Pyrite and fluorite are associated with chlorite-biotite alteration along veins and also occur in altered primary biotite sites.

At least two generations of cryptocrystalline quartz veining have taken place, often reactivating earlier biotite-chlorite veins. Cryptocrystalline quartz contains abundant sericite and/or chlorite and locally contains wall rock fragments. The most intense sericitic alteration in the wall-rock appears to be associated with the major cryptocrystalline vein; although, since there have been several stages of alteration and mineralization along the veins, it is not clear if only one stage in genetically related to the alteration.

Core 10 (1009.5-1010.7 m)

Core 10 consists of very light grey to white granite porphyry. Phenocrysts make up 40 to 60 percent of the rock and consist of approximately 20 percent euhedral orthoclase microperthite (max 1.4 cm); 20 percent equant quartz (max 1.1 cm); 5 to 10 percent plagioclase phenocrysts (max 0.7 cm) and less than 5 percent dark green-black biotite (max 0.9 cm). Groundmass is fine to medium grained, consisting of quartz and orthoclase with lesser amounts of plagioclase and biotite.

The rock is characterized by intense micro-fracturing and microbrecciation with discontinuous fractures rehealed by silica. Larger silica-filled fractures contain openings 0.1 to 0.5 cm wide. These fracture surfaces are lined with cryptocrystalline quartz and locally calcite.

In thin section, Core 10 consists of at least 50 percent phenocrysts of strongly perthitic subhedral orthoclase, subhedral embayed quartz and lesser amounts of albitic plagioclase. Plagioclase is commonly mildly altered to sericite which occurs as moderately birefringent flakes throughout the cores of the grains. The cores of some plagioclase grains have been altered to a fine-grained buff-colored aggregate of kaolinite and chlorite (?). Altered

cores of plagioclase grains locally have been replaced by microcrystalline quartz. Orthoclase is turbid, indicating incipient submicroscopic alteration.

Biotite is strongly zoned yellow-green to clear to blue-green but is brown to red-brown where abundant zircon inclusions are present. This is probably due to coalescing of pleochroic haloes around the zircon inclusions. Complex intergrowth relationships are common along grain boundaries between quartz and orthoclase and between adjacent feldspar grains. These consist mainly of fine-grained albite or quartz. Primary interstitial cavities lined by euhedral crystal faces of quartz or feldspar have been infilled with microcrystalline quartz, fluorite, muscovite, topaz or an aggregate of fine-grained kaolinite and chlorite. Trace amounts of apatite are present as well.

The rock has been intensely fractured on a macroscopic to microscopic scale with fractures rehealed by cryptocrystalline to microcrystalline quartz. Individual mineral grains are commonly fractured and rehealed by quartz, but in the larger fracture fillings, rock and mineral fragments have obviously been displaced and included within the quartz vein filling. Microfractures are generally discontinuous, horsetailing and commonly are deflected by or terminated at grain boundaries or cleavage planes, particularly where a fracture encounters a biotite grain. Locally, grains have been so intensely shattered that they are granulated. Quartz grains and fragments and biotite grains show undulatory extinction due to strain deformation in areas of intense shattering, and feldspar twinning is locally deformed.

Voids are common along larger cryptocrystalline quartz veins. Voids are lined by more coarsely crystalline quartz and are not well interconnected.

Topaz is a common accessory mineral in Core 10. Large, highly shattered topaz grains in one thin section are intergrown and infilled with orthoclase as well as microcrystalline quartz and kaolinite. A miarolitic cavity bounded by euhedral faces of topaz crystals and quartz has been partially infilled by fluorite and subsequently infilled by microcrystalline quartz.

There is no evidence for alteration directly associated with the fracture system in the Core 10 rocks in the form of alteration envelopes around quartz veins.

Core 11 (1163.4-1165.9 m)

Core 11 is a light grey, intensely brecciated and fractured granite porphyry consisting of phenocrysts of orthoclase (max. 1.1 cm), quartz (max. 1.1 cm), plagioclase (max. 0.9 cm) and biotite (max 1 cm) in a fine to medium-grained groundmass of quartz, orthoclase, plagioclase and biotite. Relative percentages of phenocrysts and groundmass are difficult to estimate in hand specimen due to the intense fracturing of the rock. Fragments of fractured phenocrysts are rehealed by quartz making phenocryst fragments difficult to distinguish from adjacent groundmass grains. Biotite is locally chloritized and feldspars are strongly kaolinized. The rock is characterized by strong silicification along discontinuous microfractures and within brecciated zones.

Along more continuous 55° to 75° veins and sheared zones, biotite appears mylonitized along vein edges and vein quartz is banded and horsetailing. Individual bands are generally discontinuous and there is evidence for repeated fracturing and rehealing of veins. Vein boundaries and silicified zones often show diffuse boundaries with country rock either by a decrease of shearing and brecciation away from the vein center or by a progressive decrease in thickness and continuity of silica-filled fractures in the brecciated zones. Some irregular and discontinuous kaolin-filled fractures are present, and kaolinite is present in some veins either as a vein filling mineral or as an alteration of feldspars incorporated in vein material and silica-filled brecciated zones.

In thin section, both groundmass and phenocryst orthoclase is strongly perthitic. Orthoclase megacrysts often contain euhedral to subhedral inclusions of quartz, plagioclase and/or resorbed orthoclase microperthite. Quartz are generally subhedral and moderately embayed. Groundmass quartz is subhedral to anhedral and interstitial. Cores of plagioclase grains are commonly strongly altered to kaolinite. Biotite occurs as phenocrysts and glomerocrysts as well as interstitially in the groundmass. Biotite is pleochroic green-brown or brown to pale yellow or yellow-green. The biotite is brown where pleochroic haloes are present around zircon inclusions.

Grain boundaries between adjacent feldspars or adjacent feldspar and quartz grains commonly contain fine-grained plagioclase and/or interstitial quartz which occurs as intergrowths with the adjacent grains or as granular aggregates along grain contacts.

Accessory minerals consist of fluorite, which is generally associated with biotite, but also fills miarolitic cavities; zircon, which occurs as inclusions within biotite; muscovite, occurring in association with biotite in miarolitic cavities; trace amounts of topaz, generally occurring along grain boundaries or in assocation with biotite and fluorite; and apatite as euhedral inclusions in quartz or feldspar grains. Miarolitic cavities are also filled with kaolinite or lined by microcrystalline quartz.

The Core 11 rocks are characterized by intense fracturing and brecciation with fractures and microbreccias rehealed by cryptocrystalline quartz. In microbreccia zones, fragments of previous silica cemented microbreccia and brecciated cryptocrystalline quartz fracture filling are contained within later cryptocrystalline vein material. Microbreccia healed by cryptocrystalline quartz is cut by a cryptocrystalline quartz vein with a sheared K-feldspar selvage. Kaolinite is associated with the bifurcating K-feldspar veining and also locally fills other fractures.

Core 12 (1297.2-1299.7 m)

Core 12 is a pale pink-grey to white fractured and brecciated granite porphyry. Approximately 50 percent phenocrysts of pale pink orthoclase orthoclase microperthite (max. 1.4 cm), quartz (max. 1.2 cm), plagioclase (max. 1.2 cm) and biotite (max. 1.0 cm) are enclosed in a pale pink very fine to fine-grained groundmass of quartz, pink orthoclase, plagioclase and minor amounts of biotite. The groundmass is finer grained and more obvious than that of Core 11. Plagioclase is strongly altered to kaolinite and orthoclase is variably altered.

Some strongly fractured and kaolinized zones are bleached white and obviously porous with both fracture porosity and microporosity within altered grains contributing to the total porosity.

The core is highly veined and brecciated with veins filled by dark grey cryptocrystalline quartz. Veins are irregular and horsetailing and thick zones may include up to 1.5 cm long fragments of the country rock. Microfractures and microbreccia, much of which is barely visible with the binocular microscope, are rehealed by silica.

In thin section, phenocryst and groundmass orthoclase is turbid. Phenocryst quartz is subhedral and strongly embayed, and groundmass quartz is equant and averages 0.45 mm. Plagioclase is commoly strongly kaolinized. Biotite is pleochroic dark brown or green brown to pale yellow, with dark brown pleochroic haloes around zircon inclusions.

Most of the rock in thin section is brecciated or fractured. Brecciated zones consist of intensely fractured wall rock cemented by microcrystalline to cryptocrystalline quartz. Microbreccia is cut by veins filled with cryptocrystalline quartz which contain wall rock and mineral fragments as well as silica cemented microbreccia fragments which have been displaced along the fracture. Fragments of cryptocrystalline quartz also are incorporated into veins. Large grains along fracture walls exhibit brittle fractures filled with cryptocrystalline silica. Away from major fractures, little if any displacement of grain fragments has taken place. In large microperthite grains, fractures generally follow cleavage planes where grain orientations are favorable. Fine fractures are generally subparallel to major fractures.

Fracture filling is dominantly cryptocrystalline quartz, but microcrystalline K-feldspar and patches of kaolinite, calcite and minoe amounts of chlorite are also present within major fracture fillings.

Core 13 (1606.3-1608.1 m)

Core 13 consists of light pink porphyritic to equigranular granite with 30 to

40 percent phenocrysts of pink orthoclase (max. 1.3 cm), quartz (max. 0.9 cm), plagioclase (up to 0.7 cm) and minor biotite (max. 0.5 cm) in a medium-grained groundmass of pink orthoclase, quartz, plagioclase and minor biotite. Average grain size of quartz and orthoclase phenocrysts is about 0.6 cm but grain size is variable and the sample locally appears equigranular. Plagioclase is moderately altered to clay minerals. Hematite staining is visible under the binocular microscope. Biotite is moderately chloritized. Miarolitic cavities averaging 0.1 cm to 0.2 cm but ranging to 0.5 cm are common.

There is no significant veining in this core, but horizontal fractures occur every 3 cm or closer, and vertical fractures are also present. No vein filling or fracture coating minerals appear to be associated with horizontal or vertical fractures. (A sample of fine-grained granite porphyry containing phenocrysts of quartz, orthoclase and biotite and cut by a 1.5 cm quartz vein was reportedly recovered at the top of this core but is not considered to have originated at this depth).

In thin section, orthoclase is turbid and strongly perthitic and sometimes contains subhedral inclusions of plagioclase. Plagioclase is more abundant than in the upper cores and is moderately zoned. A minor amount of sericite alteration was observed in some plagioclase grains. Plagioclase locally has been altered to kaolinite and/or calcite.

Biotite is slightly more abundant in Core 13 than in the upper cores. Biotite is pleochoric green-brown to yellow-green with pleochoric haloes around zircon less common than in the upper cores. Biotite is commonly partially replaced by calcite and is locally altered to chlorite, sphene and iron oxide.

Accesory minerals consist of fluorite, muscovite and calcite which occur either in association with biotite or fill miarolitic cavities. Trace amounts of zircon and apatite are also present.

Hematite staining is locally present throughout the samples.

Core 14 (1835.5-1837.6 m)

Core 14 consists of light to medium pink subequigranular granite containing approximately 45 percent pink orthoclase microperthite (max. grain size 1.4 cm), 45 percent quartz (max. 1.0 cm), 5 percent altered plagioclase (max. 0.8 cm) and 5 percent partially altered biotite (max. 0.6 cm). Horizontal fractures which occur every 8 to 10 cm have no apparent associated alteration or fracture coating. Near vertical fractures (approximately 80°) approximately 0.2 cm wide are coated with dark grey cryptocrystalline quartz. Miarolitic cavities up to 4 by 1.5 by 1 cm present in the core are lined by euhedral orthoclase and quartz crystals.

In thin section, plagioclase appears more abundant than inhand specimen. Plagioclase is altered to sericite and/or chlorite and kaolinite. The plagioclase is more altered than in Core 13, although zoning is still partially preserved. Orthoclase is strongly perthitic, and reaction rims or complex intergrowths are common at grain boundaries.

Biotite is highly altered to chlorite, sericite and opaques. Accessory minerals consist of fluorite and muscovite, with trace amounts of zircon and apatite.

A fracture system observed in thin section consists of discontinuous fractures partially rehealed by the mineral through which it passes, or filled by chlorite and sericite (muscovite?) and/or microcrystalline quartz.

In wider fracture zones, the rock has been sheared and granulated and rehealed by silica, chlorite, muscovite (sericite?) and fluorite. Quartz shows undulatory extinction in the sheared zones.

Core 15 (1953.8-1955.0 m)

Core 15 consists of light to medium pink equigranular granite made up of 50 to 55 percent pink orthoclase microperthite (up to 1.2 cm), 35 to 49 percent

quartz (up to 1.0 cm), 5 to 10 percent moderately altered plagioclase (up to 0.8 cm) and 5 percent biotite (up to 0.9 cm). Altered plagioclase is white to very pale yellow-green inhand specimen. Miarolitic cavities up to 1 by 2 cm are present throughout the core. Horizontal fractures 8 to 20 cm apart and (approximately 70°) fractures have no associated alteration and little or no surface coatings.

In thin section, grains are subhedral to anhedral. Plagioclase is mildly altered to sericite. Reaction rims are common at feldspar grain boundaries. Biotite is pleochroic green-brown to yellow-brown and is partially to completely altered to bright green chlorite,iron oxide and/or sphene. Muscovite and fluorite are common accessory minerals, generally associated with biotite, but also occurring in miarolitic cavities. Pleochroic haloes around accessory zircon inclusions in biotite are not as well developed as they are in the upper cores. A trace amount of apatite is also present in the samples.

No significant veining or fracturing is present in the thin sections of Core 15.

APPENDIX B

PHOTOMICROGRAPHS OF THIN SECTIONS OF EMPIRE CREEK GRANITE

PLATE 1 - Photomicrograph Description

A. (Core 5) Overview of texture of fresh granite porphyry (left) and granite porphyry altered to quartz-sericite rock. Groundmass quartz is subrounded with sharp grain boundaries in the fresh rock. In the quartz-sericitic rock, addition of quartz has resulted in growth of quartz grains and the formation of irregular grain boundaries. Phenocryst and groundmass feldspar has been completely altered to sericite. X20 cross-polarized light.

B. (Core 7) Overview of fabric of feldspar porphyry showing coarser groundmass texture than in Core 5 and Core 8, indicating the presence of at least two different intrusive bodies. Plagioclase feldspar commonly occurs in glomerocrysts. X20 cross-polarized light.

C. (Core 8) "Crowded" porphyry with a high ratio of phenocrysts to groundmass. Groundmass is similar in texture to Core 5 porphyry. Sieve texture and resorption are common in quartz grains. X20 cross-polarized light.

D. (Core 11) Overview showing cryptocrystalline quartz vein through shattered fine-grained porphyry. There has been some movement of mineral fragments near the core of the vein, but less movement toward the wall rock (left edge of photo). X20 cross-polarized light.

E. (Core 12) Overview of fine grained porphyry (right) cut by cryptocrystalline quartz vein. At least two episodes of fracturing and rehealing by quartz have taken place, as indicated by the finer grains size and lack of mineral fragment inclusion in the portion of the vein at the extreme left compared to the shattered zone along the vein wall.

F. (Core 15) Overview of fabric of medium to coarse grained granite porphyry. Essential minerals are orthoclase microperthite (double arrow), quartz, albite (lamellar twinned crystals) and minor biotite (single arrow). No significant alteration is present in this field of view. X20 cross-polarized light.

PLATE 1

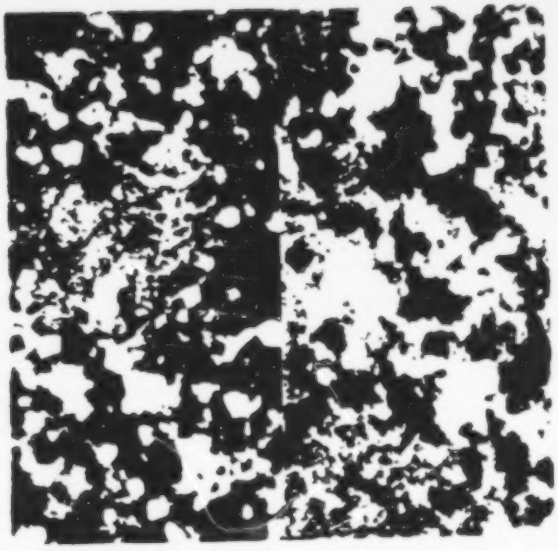

A

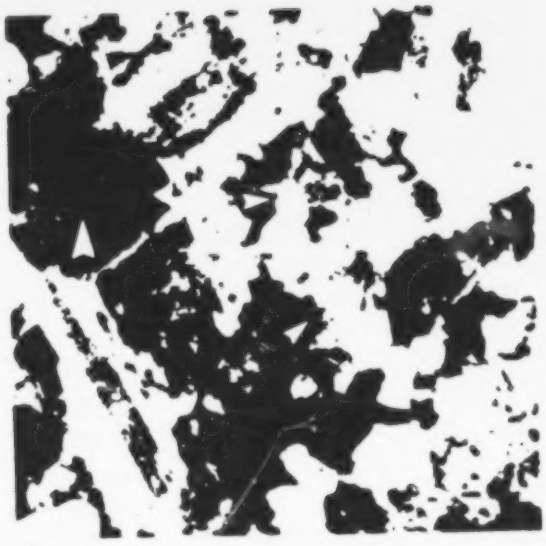

B

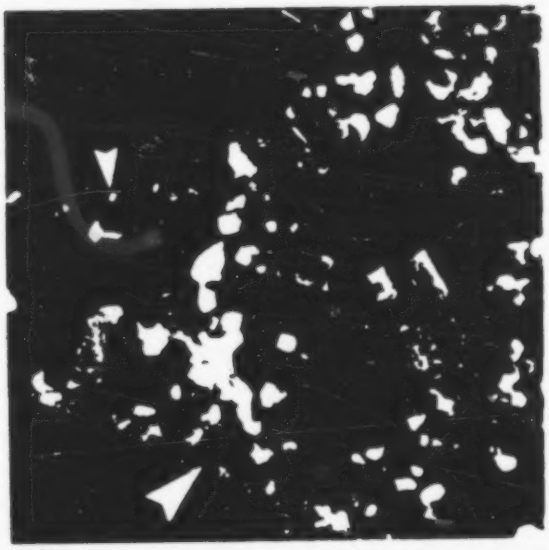

C

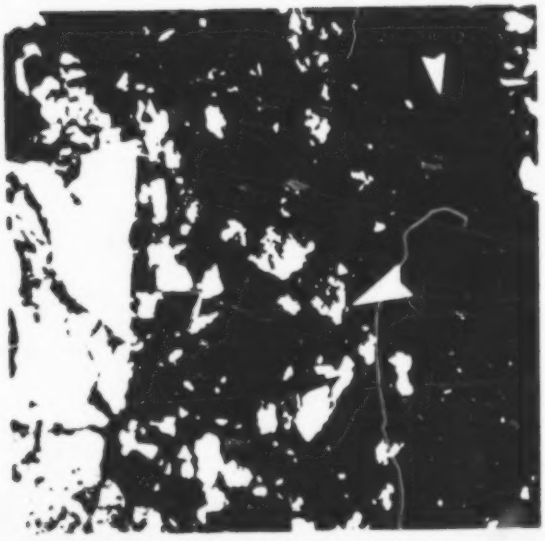

D

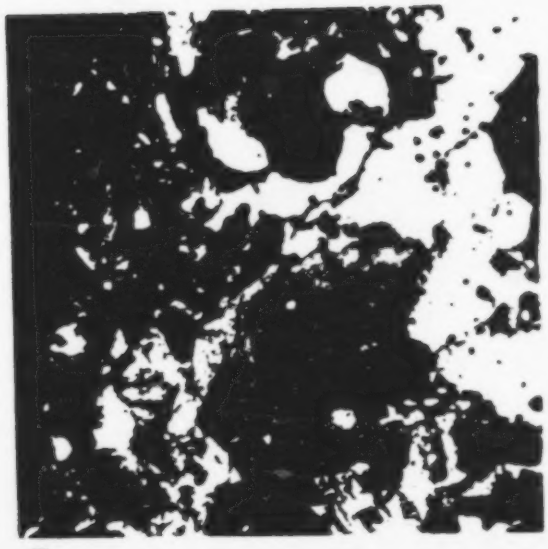

E

F

PLATE 2. Photomicrograph Description.

A. (Core 10) Open cavity (arrow) along cryptocrystalline quartz vein. Extreme shattering is not present along this fracture as is evident in fractures in Plate 1, D and E. X40 cross polarized light.

B. (Core 12) Shattered orthoclase microperthite grain infilled by silica (arrow). Shattering is not evident in many of the surrounding grains. X40 cross polarized light.

C and D. (Core 12) Same field of view shown in plane polarized light (C) and in cross polarized light (D). Detail of kaolinized (K) plagioclase phenocryst. Fracturing and rehealing by quartz (arrows) appears to have taken place after kaolinite alteration. X100.

E. (Core 12) SEM photomicrograph of porosity within a leached feldspar grain (double arrows) on a fracture surface. Microcrystal of quartz (single arrows) have precipitated on the surface of the feldspar grain. X1200.

F. (Core 12) SEM photomicrograph of kaolinite alteration within an altered plagioclase crystal. Kaolinite platelets have been corroded (arrows), possibly by circulation of hot waters. X5000.

PLATE 2

A

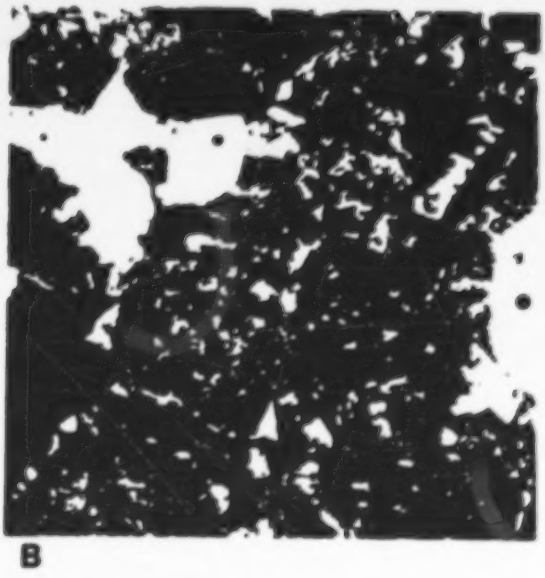

B

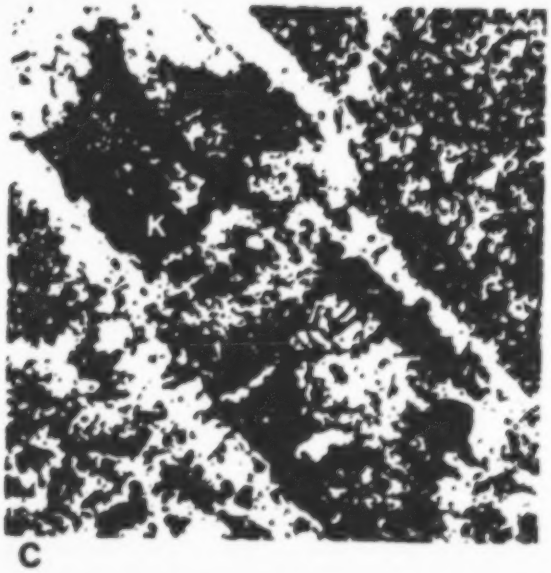

C

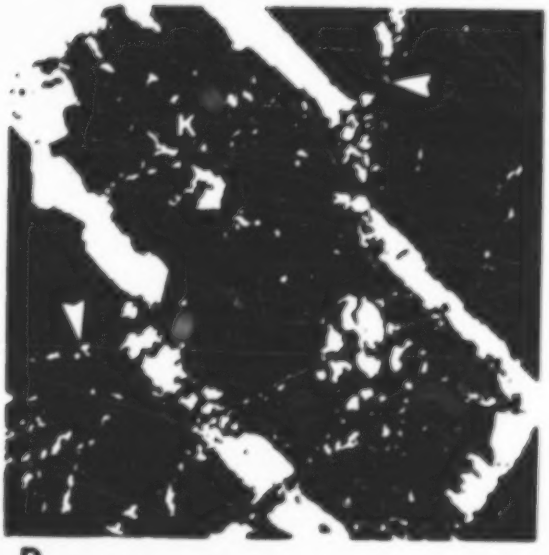

D

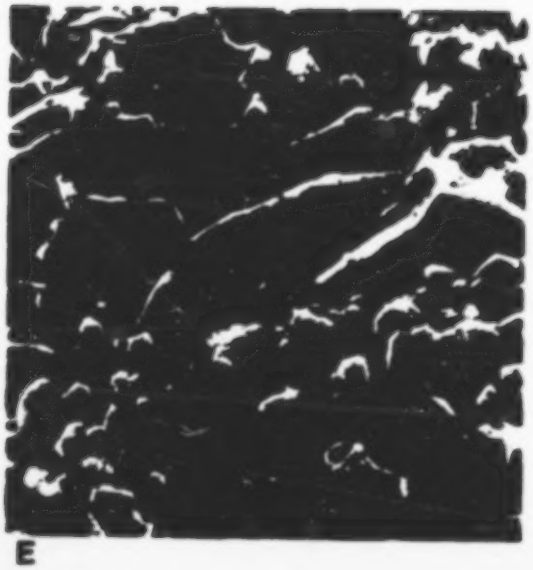

E

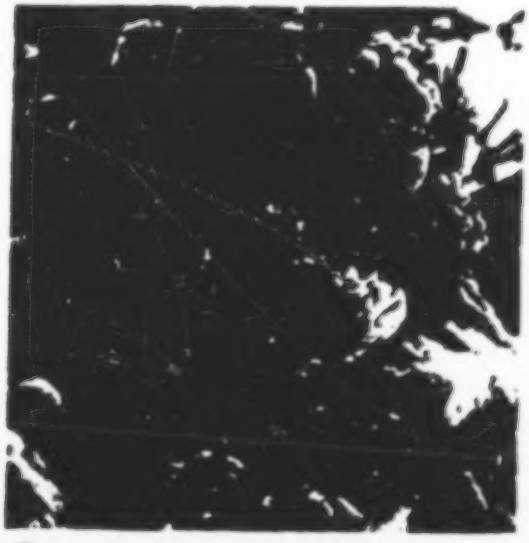

F